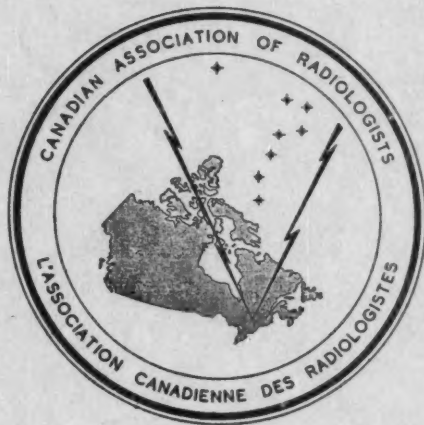


*Journal of  
the Canadian Association  
of Radiologists*



*Journal de  
l'Association Canadienne  
des Radiologistes*  
**CIRCULATION**

UNIVERSITY OF  
COLUMBIA  
JUL 21 1953  
LIBRARY

MARCH 1953 - MONTREAL

No. 1



# COBALT 60 FOR THERAPY

## NEEDLES

Linear intensities — 0.1 to 50 mc./cm.  
Active lengths — 5 to 50 mm.  
External lengths — 9 to 54 mm.  
Diameter 1.6 mm. Wall 0.3 mm.  
Bodkin eyelet. Conical point.

## TUBES

Linear intensities — 0.1 to 50 mc./cm.  
Active lengths — 5 to 20 mm.  
External lengths — 8 to 23 mm.  
Diameter 1.6 mm. Wall 0.3 mm.  
Bodkin eyelet.

## WIRE

Linear intensities — 0.1 to 8 mc./cm.  
Lengths up to 4 cm.  
Diameter 0.254 mm. (0.01 inch).

*For prices and further information  
write for descriptive bulletin CN-1.*



**ATOMIC ENERGY OF CANADA  
LIMITED**

P.O. BOX 93

OTTAWA, CANADA



## Introduct

For many years, the use of  
have been in use in  
Europe for many years.  
been described in the  
half volume of the  
work of the  
while the  
the development of  
nant to the  
equipment  
size of the  
it has been  
source of  
tem has  
may be  
and an  
minate  
makes  
to the

It has been  
calculations  
shapes of  
differences  
bers in  
in the  
The effect  
ing dis  
has been  
spite of  
clinical  
based  
unit de  
for this  
of the  
however  
in rotation

- (1) *Pro*  
*kate*
- (2) *Gr*  
*Sas*
- (3) *Dir*
- (4) *Ex*  
*Can*

# THE JOURNAL OF THE CANADIAN ASSOCIATION OF RADIOLOGISTS

Volume IV

MARCH 1953

Number 1

## A SYSTEM OF DOSIMETRY FOR ROTATION THERAPY WITH TYPICAL ROTATION DISTRIBUTIONS

H. E. JOHNS,<sup>1</sup> PH.D., F.R.S.C., G. F. WHITMORE,<sup>2</sup> B.A.,  
T. A. WATSON,<sup>3</sup> M.B., CH.B., D.M.R., and F. H. UMBERG<sup>4</sup>

Physics Dept., Saskatoon Cancer Clinic and Picker X-Ray of Canada Limited

### Introduction

For many years, X-ray rotation techniques have been used in the treatment of cancer by European workers.<sup>1-5</sup> Most of their work has been done with 200 K.V.P. equipment using half value layers of about 1 mm. Cu. In this work the patient has usually been rotated while the source has remained fixed. With the development of the high frequency resonant transformer type of X-ray generating equipment and the resulting reduction in the size of the X-ray head and connecting cables it has become possible to rotate the X-ray source about a recumbent patient. This system has certain advantages in that the patient may be more easily and securely immobilized, and any possibility of motion sickness is eliminated. The new type of equipment also makes possible rotation through any angle up to the full 360°.

It has been pointed out<sup>6</sup> that the theoretical calculations resulting for idealized body shapes and densities yield results which are different from those using ionization chambers in body cavities. Especially is this true in the region of the pelvis and oesophagus. The effect of bones and air cavities in altering distributions has long been realized and has been studied by a number of workers.<sup>7</sup> In spite of this, the fact still remains that most clinical planning for standard therapy is based on isodose distributions measured in unit density material, the only justification for this simplification being the complexity of the problem. It is reasonable to believe, however, that this problem is no more serious in rotation therapy than it is in standard fixed

field therapy. In rotation therapy there is the additional problem created by the complex shape of the body. If idealized contours are used, large errors may be introduced, especially if the tumor is eccentrically situated. In rotation therapy the focus to tumor distance (F.T.D.) and the size of the field at the tumor are the only factors which remain constant while the F.S.D., percentage backscatter, dosage rate at the skin and the amount of tissue between tumor and skin all vary. However, a comprehensive survey of the variation of depth dose with focal skin distance, surface area irradiated and quality of radiation has recently been completed in this laboratory,<sup>8</sup> and the results of this survey make possible accurate determinations of rotation distributions and form the basis of the present calculations. From this survey "tumor-air" ratios have been prepared which enable one to relate directly the dosage rate at the tumor to the output of the machine *in air*. Tables enabling one to determine the skin dose are also included. Typical distributions will be presented for tumors located in the uterine cervix, lung, oesophagus, and pituitary.

In section I "tumor-air" ratio tables will be presented and their practical use described. In section II "skin-air" ratio tables will be presented and the method by which they may be used illustrated. In section III the method by which complete distributions of radiation may be obtained will be described and illustrated by a number of examples. The physical basis and justification for the "tumor-air" and "skin-air" ratios will be presented in section IV.

### (I) "TUMOR-AIR" RATIO TABLES AND THEIR APPLICATION

#### (a) "Tumor-Air" Ratio:

In standard fixed field therapy the radiotherapist may determine the dosage rate at the tumor if the depth from the skin surface

(1) *Professor of Physics and Physicist to the Saskatchewan Cancer Commission.*

(2) *Graduate Student, Physics Dept., University of Saskatchewan.*

(3) *Director of Cancer Services for Saskatchewan.*

(4) *Executive Vice-President, Picker X-Ray of Canada, Ltd., Montreal.*



is known and a suitable isodose curve is available. In rotation therapy the tumor dose depends upon the complete contour of the patient's body and the position of the tumor with respect to this contour. As the patient rotates the entrance field size, the focal skin distance, the dosage rate on the skin all vary and the use of standard depth dose tables in obtaining the tumor dose is not possible. However, for any given field size  $A_0$  at the tumor, (Fig. 1) the dosage rate at the tumor is

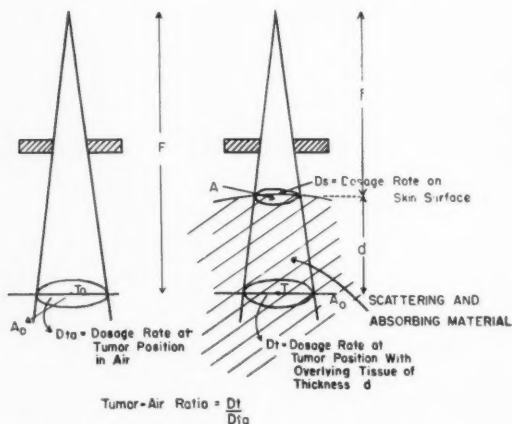


Fig. 1. Diagram to illustrate the meaning of "tumor-air" ratio.

uniquely determined by the thickness of tissue between the skin and the tumor. For this reason it is convenient to express the dosage rate at the tumor,  $D_t$ , as a ratio of the dosage rate at the tumor position with no overlying tissue between the tumor and the x-ray source. This latter dosage rate which we shall denote by  $D_{ta}$  is just the output in air of the X-ray machine when a field of area  $A_0$  is irradiated at a distance of  $F$ . The meaning of the symbols is illustrated in Fig. 1. We shall define the "tumor-air" ratio,  $R_t$  as

$$R_t = \frac{D_t}{D_{ta}} \quad (1)$$

$R_t$  is merely the ratio of the dose received in a given time by a detector placed at  $T$  to that received at  $T_a$ . The "tumor-air" ratio for a variety of field sizes, half value layers and depths of tissue has been determined from our standard depth dose tables and these are presented in Tables I and II and Fig. 2.

In Table I appear the "tumor-air" ratios for circular fields and in Table II data for rectangular fields; in both cases the field size is the size at the tumor position. "Tumor-air" ratios are independent of Focal Tumor Distance  $F$  over the range of  $F$  from 40 to 100

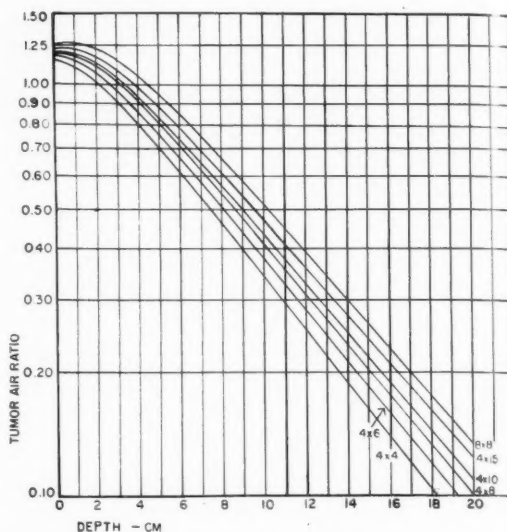


Fig. 2. "Tumor-air" ratio curves. Graph showing the "tumor-air" ratio as a function of depth for a number of rectangular fields. Half value layer 2 mm. Cu. focal tumor distances 40 to 100 cm.

cm. Some of the data for rectangular fields is plotted in Fig. 2. The curves are not unlike depth dose curves when these are referred to air. It is clear from Fig. 2 that for zero depth the "tumor-air" ratio is merely the backscatter factor. "Tumor-air" ratios may be used in rotation therapy in much the same way as depth dose data may be used in standard therapy. They are, however, very different quantities. The method by which they were obtained will be discussed later; in the meantime, their use will be illustrated.

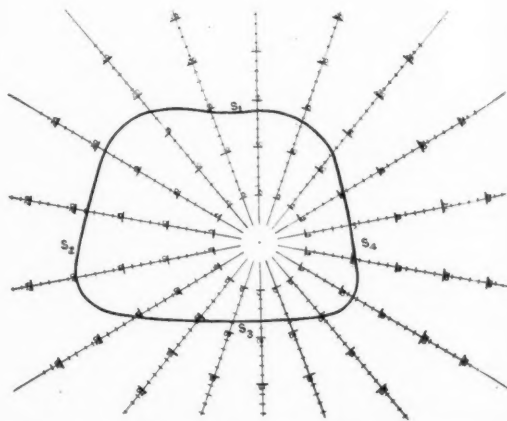


Fig. 3. Apparatus for determining the body contour and the distance of the tumor from the skin for a number of equally spaced radii.

**TABLE I**  
**"TUMOR-AIR" RATIOS FOR CIRCULAR**  
**FIELDS H.V.L. 1.0**

(These apply to focal tumor distances  
from 40 to 100 cm.)

Half Value Layer 1.0 mm. Cu.

Area Depth	0	20	35	50	80	100
0	1.000	1.19	1.24	1.280	1.34	1.37
2	0.682	1.07	1.17	1.240	1.33	1.37
4	0.472	0.836	0.940	1.02	1.13	1.19
6	0.330	0.625	0.720	0.794	0.900	0.957
8	0.232	0.462	0.541	0.607	0.694	0.744
10	0.163	0.338	0.402	0.448	0.525	0.569
12	0.114	0.244	0.291	0.336	0.398	0.432
14	0.079	0.176	0.216	0.248	0.298	0.324
16	0.055	0.127	0.157	0.182	0.224	0.244
18	0.039	0.092	0.115	0.134	0.166	0.182
20	0.027	0.066	0.083	0.098	0.124	0.137

Half Value Layer 2.0 mm. Cu.

Area Depth	0	1.00	1.16	1.20	1.24	1.28	1.31
0	1.00	1.16	1.20	1.24	1.28	1.31	1.31
2	0.720	1.05	1.14	1.20	1.27	1.30	1.30
4	0.515	0.835	0.928	1.00	1.09	1.15	1.15
6	0.372	0.642	0.733	0.805	0.896	0.940	0.940
8	0.268	0.485	0.563	0.623	0.717	0.755	0.755
10	0.193	0.361	0.428	0.480	0.558	0.601	0.601
12	0.140	0.270	0.323	0.368	0.433	0.468	0.468
14	0.102	0.201	0.244	0.276	0.331	0.360	0.360
16	0.073	0.149	0.183	0.210	0.253	0.279	0.279
18	0.054	0.111	0.138	0.159	0.195	0.214	0.214
20	0.039	0.084	0.105	0.120	0.148	0.164	0.164

Half Value Layer 4.0 mm. Cu.

Area Depth	0	1.000	1.13	1.16	1.18	1.21	1.22
0	1.000	1.13	1.16	1.18	1.21	1.22	1.22
2	0.750	1.04	1.09	1.12	1.17	1.19	1.19
4	0.562	0.845	0.917	0.965	1.03	1.06	1.06
6	0.430	0.661	0.733	0.782	0.860	0.890	0.890
8	0.328	0.519	0.573	0.624	0.692	0.727	0.727
10	0.249	0.398	0.449	0.491	0.555	0.587	0.587
12	0.191	0.308	0.350	0.384	0.436	0.466	0.466
14	0.146	0.238	0.272	0.300	0.344	0.368	0.368
16	0.112	0.183	0.210	0.232	0.271	0.293	0.293
18	0.086	0.141	0.164	0.181	0.214	0.230	0.230
20	0.067	0.110	0.127	0.140	0.167	0.182	0.182

**TABLE II — "TUMOR-AIR" RATIOS — RECTANGULAR FIELDS**

(These apply to focal tumor distances 40 - 100 cm.)

Half Value Layer — 2.0 mm. Cu.

Depth	4x4	4x6	4x8	4x10	4x15	6x6	6x8	6x10	6x15	5x5	8x8	10x10
0	1.14	1.17	1.19	1.20	1.22	1.21	1.23	1.25	1.28	1.18	1.26	1.31
1	1.10	1.15	1.19	1.20	1.22	1.21	1.23	1.25	1.31	1.15	1.27	1.32
2	1.02	1.07	1.12	1.13	1.17	1.14	1.18	1.22	1.25	1.08	1.23	1.30
3	0.905	0.959	1.01	1.03	1.07	1.04	1.09	1.13	1.17	0.971	1.15	1.24
4	0.799	0.851	0.901	0.930	0.970	0.935	0.985	1.03	1.07	0.868	1.05	1.15
5	0.705	0.755	0.805	0.823	0.870	0.837	0.884	0.930	0.970	0.766	0.945	1.05
6	0.611	0.662	0.708	0.730	0.774	0.738	0.785	0.831	0.870	0.675	0.844	0.936
7	0.531	0.578	0.624	0.643	0.690	0.653	0.696	0.741	0.779	0.591	0.754	0.843
8	0.460	0.504	0.545	0.565	0.605	0.570	0.611	0.655	0.695	0.515	0.663	0.757
9	0.396	0.438	0.470	0.492	0.531	0.497	0.536	0.577	0.616	0.445	0.583	0.672
10	0.340	0.378	0.410	0.429	0.465	0.432	0.469	0.508	0.543	0.385	0.511	0.596
11	0.295	0.329	0.355	0.375	0.407	0.375	0.408	0.444	0.477	0.336	0.448	0.527
12	0.255	0.284	0.310	0.328	0.357	0.327	0.358	0.388	0.421	0.289	0.394	0.465
13	0.219	0.246	0.269	0.284	0.313	0.283	0.310	0.340	0.370	0.250	0.344	0.408
14	0.189	0.214	0.234	0.247	0.274	0.247	0.272	0.297	0.325	0.216	0.300	0.358
15	0.162	0.184	0.203	0.215	0.240	0.214	0.235	0.259	0.285	0.188	0.261	0.316
16	0.140	0.160	0.175	0.187	0.210	0.185	0.206	0.226	0.250	0.162	0.228	0.277
17	0.121	0.138	0.154	0.164	0.183	0.161	0.178	0.197	0.221	0.141	0.200	0.242
18	0.104	0.120	0.133	0.143	0.162	0.139	0.156	0.172	0.193	0.122	0.174	0.213
19	0.090	0.104	0.116	0.124	0.141	0.122	0.136	0.150	0.171	0.105	0.152	0.188
20	0.078	0.088	0.101	0.109	0.125	0.105	0.118	0.131	0.149	0.092	0.132	0.164

### (b) Application of "Tumor-Air" Ratio

For each patient it is only necessary to calculate the dosage rate at the tumor once detailed isodose distributions for the "average" patient for the site in question have indicated the suitability of the technique. In the calculation the following steps should be carried out.

- (1) The contour of the patient in the plane of the tumor should be determined. A number of devices have been designed for this purpose.<sup>9</sup> One particularly useful method makes use of a heavy lead wire or piece of solder which may be made to conform to the body contour. This contour can then be laid over a polar diagram with the tumor at the pole as illustrated in Fig. 3 for a tumor of the lung, the position of the tumor inside the contour having been previously determined. The polar diagram can readily be constructed on a piece of cardboard.
- (2) The distance from the tumor to the skin surface for a number of equally spaced radii may now be read off directly. These are shown in Table III. The "tumor-air" ratios are obtained from Fig. 2 and entered as the third column of Table III. The mean of these is 0.377.
- (3) Suppose now that the output of the machine in air is 50r/min. at a distance of 60 cm. and that the tumor was placed 60 cm. from the focal spot, then the dosage rate at the tumor is  $50 \times 0.377 = 18.9$  r/min. The total time required to deliver any desired tumor dose may now be evaluated. During this treatment time an integral number of rotations should be made.

(4) In many cases the procedure of (2) and (3) may be simplified if the body contour approximates a circle with the tumor at the centre. The radii must still be measured but now the "tumor-air" ratio need be evaluated for only the mean radius. In the above case the mean radius is 13.0 and the corresponding "tumor-air" ratio 0.343. This is about 10 percent different from the accurate "tumor-air" ratio and in this case the short cut would not be justified. In Table IV is given the same type of calculation for a cancer of the mid-oesophagus. The mean "tumor-air" ratio is now 0.379 and the "tumor-air" ratio obtained from the mean radius 0.374. Certainly in this case a knowledge of the mean radius is all that is required. The agreement is good because the tumor is near the centre of the skin contour. In this particular case it is only necessary to measure the radii for one-half of the body ( $0^\circ - 180^\circ$ ) because of the symmetry.

TABLE III

## CALCULATION OF TUMOR DOSE FOR CANCER OF THE LUNG

Field size 8 x 8 at tumor. H.V.L. 2.0 mm. Cu.

Angle	Radius (cm)	"Tumor-air" Ratio (R <sub>2</sub> )
0	13.7	0.310
20	14.5	0.279
40	17.7	0.182
60	18.8	0.157
80	18.5	0.163
100	19.7	0.138
120	15.7	0.238
140	10.6	0.475
160	8.9	0.584
180	8.8	0.600
200	9.4	0.550
220	10.4	0.488
240	11.6	0.415
260	10.4	0.488
280	10.1	0.508
300	10.2	0.501
320	11.8	0.404
340	13.4	0.324
Mean	13.0	0.377
Mean "tumor-air" ratio		0.377
"Tumor-air" ratio using the mean radius of 13.0 cm.		0.343

TABLE IV

## CALCULATION OF TUMOR DOSE FOR CANCER OF THE OESOPHAGUS

Field size 15 x 6 cm. at tumor. Half Value Layer  
2.0 mm. Cu.

Angle	Radius	"Tumor-Air" Ratio
0	10.7	0.499
20	11.8	0.433
40	13.4	0.355
60	13.7	0.337
80	13.5	0.351
100	14.8	0.292
120	16.6	0.225
140	13.8	0.337
160	11.4	0.461
180	10.7	0.499
Mean	13.0	0.379
Mean "tumor-air" ratio		0.379
"Tumor-air" ratio using the mean radius of	13.0	0.374

## II — "SKIN-AIR" RATIO TABLES AND THEIR APPLICATION

After the patient, or X-ray machine, has made one complete rotation each point on the patient's skin will have been given a definite

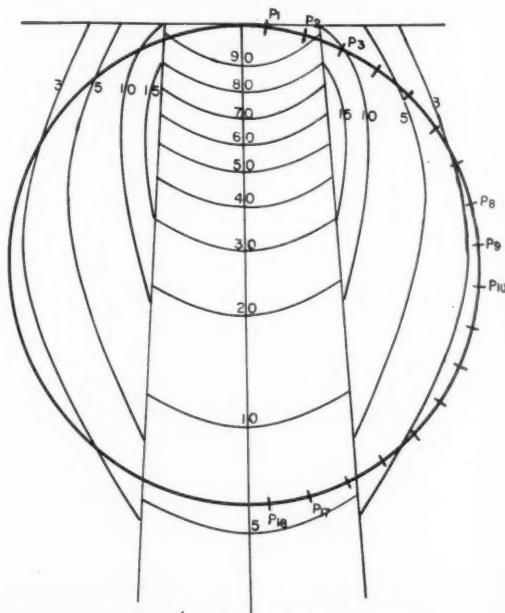


Fig. 4. Diagram showing the method of calculating the skin dose for a circular phantom. The field is directed towards a tumor at the centre of the circle.



dose. However, this dose is very difficult to determine accurately for it will depend on the complete contour of the body. If for the moment we assume that the contour of the body is a circle centred on the tumor then each point on the skin surface in the plane of rotation receives the same dose and this can be determined. Consider Fig. 4 which shows a typical isodose curve directed towards the centre of a circle where the tumor is located. The doses at points  $P_1, P_2$  — to  $P_n$  may be read off Fig. 4. The dose received at any of these points after a complete rotation is the average of the doses at points  $P_1$  to  $P_n$ . This average dose has been expressed as a ratio of the dose in air at the tumor position and we call this ratio the "skin-air" ratio ( $R_s$ )

$$R_s = \frac{\text{Average dose } P_1 \text{ to } P_n}{\text{Dose received in air at Point T}} \quad (2)$$

This ratio has been determined for Focal Tumor Distance of 60 cm. for a selection of rectangular fields and for phantom radii from 6 to 16 cm. and these are presented in Table V. In all cases the long dimension of the rectangular field is parallel to the axis of rotation and the field sizes refer to the size at the centre of the circle, i.e., the tumor position.

Suppose a circular body of radius 12 cm. with a tumor at its centre is treated using a field of  $15 \times 6$  cm. at the tumor position and a focal tumor distance of 60 cm. Suppose the output of the machine at the tumor position in air is 50r/min. From Table V the "skin-air" ratio is 0.175. The dosage rate on the skin is, therefore,  $0.175 \times 50 = 8.8$  r/min. "Skin-air" ratios are thus used in exactly the same way as "tumor-air" ratios.

It is immediately evident from Table V that the smallest "skin-air" ratios are obtained using narrow fields. For example, we see that the "skin-air" ratio for an  $8 \times 8$  field and phantom radius 12 cm. is 0.211 as compared with 0.101 for an  $8 \times 4$  field. In general, for a given series of fields such as  $10 \times 4, 10 \times 6, 10 \times 8, 10 \times 10$  the "skin-air" ratio is proportional to the small dimension of the field. This points up a well known fact that for minimum skin dose the field should be made as narrow as the width of the tumor will permit.

The "skin-air" ratios of Table V depend somewhat on the focal tumor distance, although the dependence is not great. For these reasons Table V may be used with reasonable accuracy for focal tumor distances from 50 to 100 cm. The dependence of "skin-air" ratios on F.S.D. will be discussed in detail in section IV.

In practice the body contour is seldom a circle. However, the results of Table V may be used to predict to an accuracy of about 10 per cent the dose on the skin for any given clinical condition. Suppose, for example, we wish to determine the skin dose at points  $S_1, S_2, S_3$  and  $S_n$  of Fig. 3. Pertinent information is given in Table VI. The last column gives the dosage rate at the skin as determined accurately by the method of the next section.

It is seen that the predicted skin doses are somewhat higher than the actual ones for points  $S_1, S_2$ , and  $S_3$ , but lower for  $S_n$ . In general the method will overestimate the dose at skin points near the tumor and underestimate the skin points a long distance from the tumor. As the body contour approaches a

TABLE V  
"SKIN-AIR" RATIOS  
Half Value Layer 2.0 mm. Cu.  
Focal Tumor Distance 60 cm.  
Field Sizes at the Tumor

Radius Phantom	4x4	4x6	4x8	4x10	4x15	5x5	6x6	6x8	6x10	6x15	8x8	10x10
6	0.210	0.220	0.231	0.240	0.265	0.271	0.338	0.351	0.365	0.400	0.500	0.649
7	0.166	0.177	0.188	0.199	0.218	0.223	0.278	0.292	0.303	0.335	0.411	0.541
8	0.142	0.152	0.161	0.169	0.183	0.186	0.233	0.248	0.260	0.286	0.345	0.457
9	0.124	0.132	0.140	0.146	0.156	0.159	0.203	0.215	0.226	0.250	0.297	0.395
10	0.108	0.117	0.124	0.130	0.136	0.140	0.179	0.190	0.200	0.217	0.260	0.350
11	0.097	0.105	0.112	0.117	0.122	0.125	0.159	0.170	0.178	0.195	0.233	0.313
12	0.087	0.094	0.101	0.106	0.110	0.113	0.142	0.151	0.159	0.175	0.211	0.284
13	0.078	0.085	0.091	0.096	0.100	0.102	0.128	0.135	0.142	0.157	0.192	0.258
14	0.071	0.078	0.084	0.088	0.092	0.093	0.116	0.123	0.128	0.144	0.177	0.236
15	0.065	0.071	0.076	0.080	0.084	0.085	0.106	0.112	0.117	0.131	0.162	0.217
16	0.060	0.065	0.070	0.074	0.077	0.078	0.097	0.103	0.107	0.120	0.149	0.200

Approximate Correction Factors for other Half Value Layers	1.0	3.0	4.0	H.V.L. - mm. Cu.
	1.03	0.980	0.960	Correction Factor

circle with the tumor at its centre, the overall agreement will improve. Since, for most purposes, a rough estimate of the skin dose is all that is required in rotation therapy, the "skin-air" ratio concept is useful.

TABLE VI

Comparison of Skin Doses as calculated accurately and by the use of "Skin-Air" Ratios

(Assume a dosage rate in air of 50r/min. at the tumor position and an 8 x 8 field at a focal tumor distance of 60 cm.)

Points (see Fig. 3)	Radius (Distance from tumor)	"Skin-Air" Ratio 8 x 8 field	Dose rate on skin r/min.	
			Approximate from "Skin-air" Ratio	From complete distribution (Fig. 7)
S <sub>1</sub>	13.7	0.181	9.1	8.6
S <sub>2</sub>	19.0	0.127	5.5	6.2
S <sub>3</sub>	8.0	0.345	17.2	15.1
S <sub>4</sub>	10.0	0.260	13.0	11.9

### III — COMPLETE DISTRIBUTIONS OF RADIATION

In sections I and II we have shown how the tumor dose and the skin dose may be determined under any clinical conditions of rotation therapy. We must now determine the dosage rate at other points in the phantom to see if a suitable distribution of radiation is obtained. Calculations of this kind are very involved and time consuming but the method will be discussed and typical distributions obtained for a number of examples. In what follows the contour for an "average patient" has been taken from Eycleshymer and Schoemaker's cross section anatomy.<sup>10</sup> In practice a complete distribution of radiation would not be required for each patient provided detailed calculations based on an "average patient" have shown that a suitable distribution may be obtained.

#### (a) Calculation of Complete Rotation Distributions:

The isodose curves used in the determination of the clinical distributions were calculated from our depth dose survey for circular fields using the method developed initially by Clarkson<sup>11</sup> and subsequently by Meredith and Neary<sup>12</sup>. In this method one determines the effect of primary and secondary radiation separately at a number of points within the phantom. Inside the beam defined by the limiting diaphragm, the radiation is composed of both primary and secondary radiation, while outside the geometric edge of the beam there is secondary only. The primary radiation for any depth is obtained directly from the depth dose survey for zero area. The amount of scattered radiation for any point

is determined from the survey by analysing the manner in which the depth dose varies with the size of the circular field. This has been done by a graphical method similar to that first discussed by Clarkson.<sup>11</sup> With this method, isodose distributions for any shaped fields may be obtained from the standard depth dose tables. In Fig. 5 are shown two isodose distributions for half value layer of 2 mm. of Cu., using a focal tumor distance of 60 cm. and a field size of 8 x 8 cm. at this tumor distance. The distribution on the left is produced when there is 20 cm. between the tumor point and the skin S. The focal skin distance is thus 40 cm. and the field size at the surface of the skin 5.3 x 5.3 cm. The distribution on the right corresponds to a tissue depth of 10 cm. (S<sub>2</sub> T = 10 cm.) and hence a focal skin distance of 50 cm. The field size at the skin is now 6.6 x 6.6 cm. The two distributions are quite different and it is evident that appreciable errors can be introduced in assuming a fixed body radius and hence isodose distributions, in cases where the axis of rotation is eccentrically situated in the body.

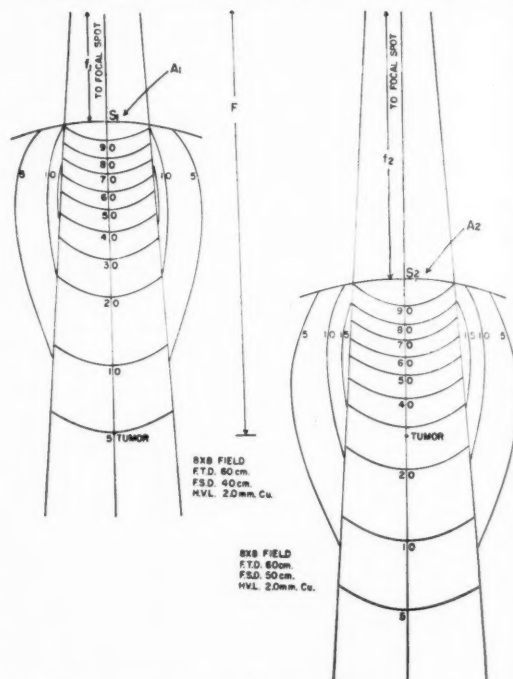


Fig. 5. Two isodose distributions both giving a field of 8 x 8 cm. at focal tumor distance of 60 cm. For the one on the left there is 20 cm. of tissue between the skin surface and the tumor. The focal skin distance is therefore 40 cm. and the area of the entrance field is 5.3 x 5.3 cm. For the distribution on the right there is 10 cm. of tissue between the skin and tumor. The focal skin distance is 50 cm. and the entrance field is 6.6 x 6.6 cm. H.V.L. 2.0 mm. Cu.

Although the skin doses for both fields of Fig. 5 are marked as 100, the absolute doses received by the points  $S_1$  and  $S_2$  in a given length of time are, of course, quite different. The Dosage rate at  $S_2$  ( $D_{s_2}$ ) is decreased from

that at  $S_1$  ( $D_{s_1}$ ) by the factor  $\frac{(f_1)^2}{(f_2)^2}$  due to the

inverse square law, but it is increased slightly by a factor depending on the percentage backscatter. The area of the field at  $S_1$  (i.e.  $A_1$ ) is smaller than  $A_2$  hence the backscatter  $b_1$  is smaller than  $b_2$ . The ratio of the dosage rate  $D_{s_2}$  to the dosage rate  $D_{s_1}$  is given by the

$$\text{Correction Factor} = \frac{D_{s_2}}{D_{s_1}} = \frac{(f_1)^2}{(f_2)^2} \frac{(1 + b_2)}{(1 + b_1)} \quad (3)$$

The inverse square law factor  $\frac{(f_1)^2}{(f_2)^2}$  differs considerably from 1.0 in this case, being 0.64 while the second factor depending on backscatter is almost constant and equal to 1.0, in this case 1.031. The total factor given by equation (3) for the arrangement shown in Fig. 5 is  $0.64 \times 1.031 = 0.66$ . In many cases where the tumor is situated near the centre of a nearly circular body shape the factor  $(1 + b_2)/(1 + b_1)$  may be taken as equal to 1.0.

In Fig. 6 is shown the contour of the chest. It is desired to obtain the resultant distribution produced by rotation about an axis through T using an  $8 \times 8$  field at a focal tumor distance of 60 cm. On the body contour a number of points such as  $P_1, P_2$ , etc., where the dose is to be determined, were chosen. It

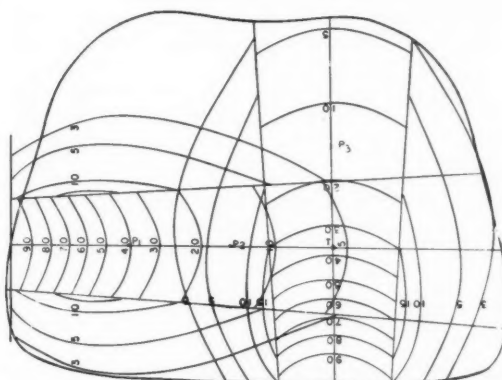


Fig. 6. Shows a contour of the chest wall. Superimposed on this contour are the two distributions of Figure 5. These give a field size of  $8 \times 8$  cm. at the tumor. H.V.L. 2 mm. of Cu.

is convenient to choose these points at equal angular intervals around circles centered at the tumor. Through the tumor T a series of radii at  $20^\circ$  intervals were drawn. (These are not shown in Fig. 6). The appropriate isodose curves were then superimposed over the body contour and the dose contributions received at the selected points P read off. The appropriate isodose curve for the next position was then overlaid on the next diameter position and the same procedure followed. Two typical positions of the isodose curves are shown in Fig. 6. In determining the dose at the selected points the average dose over a twenty

TABLE VII  
Showing the Method by which the Doses at Points  
 $P_1, P_2, P_3$ , and T of Fig. 6 may be determined

Angle of Incidence	Body Radius	F.S.D.	$\frac{(f_1)^2(1+b_2)}{(f_2)^2(1+b_1)}$	Percentage Dose Contributions to $P_1, P_2, P_3$ & T				Dose Contributions to $P_1, P_2, P_3$ & T.			
				$P_1$	$P_2$	$P_3$	T.	$P_1$	$P_2$	$P_3$	T.
0	13.7	46.3	1.03	1.5	4.0	38.0	15.0	1.5	4.1	39.2	15.5
20	14.5	45.5	1.05	1.5	3.5	30.0	13.5	1.6	3.7	31.5	14.2
40	17.7	42.3	1.21	2.0	5.0	10.0	7.5	2.4	6.1	12.1	9.1
60	18.8	41.2	1.28	5.0	12.5	3.0	6.5	6.4	16.0	3.8	8.3
80	18.5	41.5	1.26	39.0	16.0	2.5	7.0	49.1	20.2	3.2	8.8
100	19.7	40.3	1.35	27.0	13.0	2.0	5.0	36.4	17.5	2.7	6.7
120	15.7	44.3	1.12	5.0	22.0	3.0	11.5	5.6	24.6	3.4	12.9
140	10.6	49.4	0.915	2.1	13.0	10.5	27.0	1.9	11.9	9.6	24.7
160	8.8	51.2	0.835	1.3	8.8	14.0	36.0	1.1	7.4	11.7	30.1
180	9.0	51.0	0.840	1.5	8.0	16.0	40.0	1.3	6.7	13.4	33.6
200	10.4	49.6	0.905	1.5	7.5	14.0	36.0	1.4	6.8	12.7	32.6
220	11.6	48.4	0.942	1.5	8.5	10.5	28.0	1.4	8.0	9.9	26.4
240	10.4	49.6	0.905	2.0	9.5	6.0	23.0	1.8	8.6	5.4	20.8
260	9.8	50.2	0.883	4.2	11.5	6.5	28.0	3.7	10.1	5.7	24.7
280	10.1	49.9	0.895	5.0	13.5	8.0	32.0	4.5	12.1	7.2	28.6
300	10.2	49.8	0.887	2.4	12.0	10.0	30.0	2.1	10.6	8.9	26.6
320	11.8	48.2	0.950	1.3	8.0	25.0	22.5	1.2	7.6	23.8	21.4
340	13.4	46.6	1.01	1.5	5.0	38.0	17.5	1.5	5.1	38.4	17.7
Mean	13.0 cm.	47.0 cm.		Total				124.9	187.1	242.6	362.7
				% Depth Dose				34.4	51.6	66.9	100

degree arc centred about the point is recorded. Where the point is well inside or outside the edge of the beam the dose at the point may be taken as equal to the average over the interval, but when the point is near the geometric edge of the beam the average dose over the interval is obtained by inspection.

The above method is illustrated in Table VII. In the first column appear the angles of incidence of the X-ray beam measured from the zero direction shown in Fig. 6. In the second columns appear the radii, of the body at each  $20^\circ$  position. The average body radius is shown at the bottom and is 13.0 cm. The focal skin distance listed in column 3 is the difference between the focal tumor distance and the body radius. The fourth column gives the correction factor of equation (3). In this expression,  $f_1$  was placed equal to 47 (the average focal skin distance corresponding to a mean body radius of 13.0) and  $b$  was taken as the percentage backscatter for the field size at F.S.D. 47 cm. The next four columns give the dose contributions from each  $20^\circ$  degree interval for the points  $P_1$ ,  $P_2$ ,  $P_3$  and  $T$ , for a dose of 100r to each skin surface. These were obtained as indicated above, and can be read off Fig. 6 for the angular positions  $90^\circ$  and  $180^\circ$ . The contributions for the other angles are obtained from the appropriate overlays. Finally the last four columns contain the dose contributions for the same four points corrected for the variation in the skin dose. They are obtained by multiplying the percentage depth dose values by the correction factor of column 4. These values correspond to the dose received at the points,  $P_1$ ,  $P_2$ ,  $P_3$  and  $T$  when a dose of 100r with backscatter has been given at F.S.D. 47 cm. At the bottom of the table these corrected contributions have been totalled and expressed as a percentage of the tumor dose. We see, for example, that after a complete rotation, point  $P_1$  receives 34.4 per cent of the dose received at the tumor  $T$ . The distribution shown in Fig. 7 for a lung tumor eccentrically situated treated using  $360^\circ$  degree rotation, was obtained in this way. We note that the highest skin dose is 80 per cent of the tumor dose and that it occurs at the point where the skin is closest to the tumor. We also observe that the tumor  $T$  is not situated at the centre of the 100% isodose curve. Although the beams were always directed towards  $T$  during rotation a slightly higher dose occurs at points somewhat nearer the nearest skin surface. This is an illustration of the well known principle in fixed field therapy that when beams are directed through one surface of a patient towards a tumor they should be directed to a point somewhat below the tumor

in order that the maximum dose occur at the tumor. In Fig. 7 a somewhat better distribution about  $T$  would have been obtained had the rotation been made about a point 2 cm. above and to the left of  $T$ .

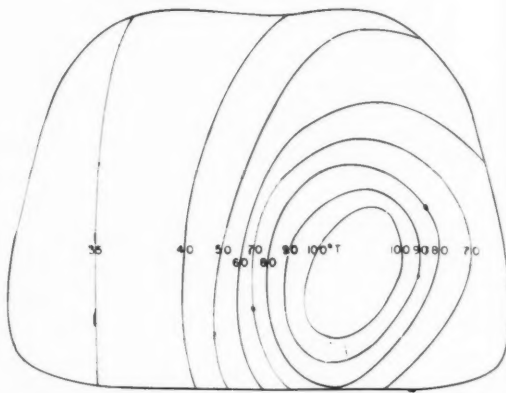


Fig. 7. Resultant distribution obtained by  $360^\circ$  rotation about a tumor of the lung at  $T$ . Field size of tumor  $8 \times 8$  cm., focal tumor distance 60 cm. H.V.L. 2 mm. of Cu.

The method outlined above to obtain a complete rotation distribution can be made as accurate as one desires but, unfortunately, it is very time consuming. However, in many cases certain simplifying approximations can be made. If the body contour approximates a circle, only one isodose curve for the corresponding focal skin distance need be constructed. This is certainly valid when the radius vector does not vary by more than two or three centimeters from the average value. Over this range the isodose curves do not change appreciably since they are an insensitive function of the focal skin distance and the area of the field. However, even if the variations in radii are not great it is essential that the dose from each angle be multiplied by the inverse square factor. When the variation in radii is small the exact distribution is not very different from that obtained assuming a circular body contour. The small difference is illustrated in Fig. 8 which will be discussed later.

So far we have considered rotation through  $360^\circ$ . The method, however, applies equally well to smaller angles of rotation. The machine should be rotated so that the axis of the beam moves at a uniform angular velocity from one limiting point to the other and then reverses its direction. If this is not possible the machine can be set for  $360^\circ$  rotation and the shutter opened and closed at the appropriate places. The use of lead shielding on

the sk  
of rot  
for as  
the an  
finally

(b) T

The  
tions  
outlin  
assum  
and a  
bodies



Fig. 8. combining summing. Rotation from omitted contour at a focal distance of Cu.

Fig  
radius  
tained  
 $220^\circ$  a  
on ea  
latera  
with  
distrib  
the bo  
cles o  
B on  
shape  
the le  
the r  
space  
right  
tion o  
using  
circul  
is ins



the skin surface to obtain the required angle of rotation complicates the problem greatly for as the beam crosses the lead diaphragm, the area of the field is reduced in width and finally is cut off altogether.

### (b) Typical Distributions

The accompanying diagrams show distributions which were obtained using the methods outlined above. In all these examples we assumed a half value layer of 2.0 mm. of Cu. and a focal tumor distance of 60 cm. and bodies of unit density.

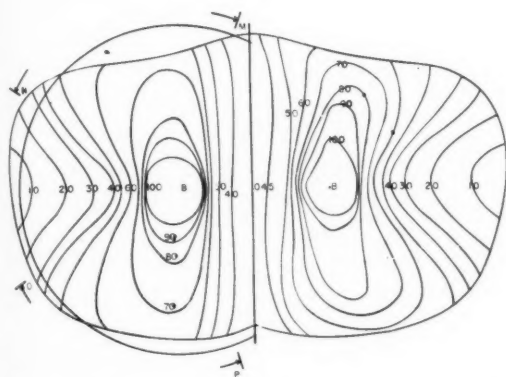


Fig. 8. The left-hand distribution was obtained by combining rotations about the two points B, assuming the body surface to be circular as indicated. Rotation was from M to P with the shutter closed from N to O. That is,  $220^\circ$  rotation with  $60^\circ$  omitted. The rotation distribution on the right was obtained in the same way except the actual body contour was used. The field size at B was  $10 \times 4$  at a focal tumor distance of 60 cm. H.V.L. 2 mm. of Cu.

Fig. 8 gives the distributions for post-radium treatment of cancer of the cervix obtained using a  $10 \times 4$  cm. field and a rotation of  $220^\circ$  about the point B (Tod and Meredith<sup>13</sup>) on each side and omitting an arc of  $60^\circ$  in the lateral position, i.e., rotation from M to P, with the X-rays shut off from N to O. The distribution on the left results from assuming the body contour to be composed of two circles of radius 10.5 cm. centred at the points B on each side. The assumed circular body shape is shown. The distribution shown on the left is the resultant obtained by combining the rotations about both points B. To save space only the left hand side is shown. The right side would be identical. The distribution on the right side of Fig. 8 was obtained using the actual body contour instead of the circular one. The difference between the two is insignificant, indicating that when the

body shape over the angle of rotation desired approximates a circle, a circular contour may be assumed with no great error. For both distributions, the ratio of the tumor dose to the maximum skin dose is about 1.4 : 1. The omission of the  $60^\circ$  lateral segment reduces the amount of radiation reaching the cervix in the body centre which is assumed treated with intra-cavitary radium using the Manchester system.<sup>14</sup> The omission of these segments also reduces the amount of radiation absorbed by the heads and necks of the femurs. If this is not done the poorer distribution of Fig. 9 is obtained.

The left half of Fig. 9 gives the total distribution to one-half of the body resulting from the use of a  $10 \times 4$  cm. field and  $180^\circ$  arc of rotation about each of the points B, i.e., rotation from M to N. The right side of the same figure gives the distribution obtained under identical conditions but with a rotation of  $220^\circ$ , i.e., from O to P. In both cases the X-ray dosage received at the centre of the body is approximately 50 per cent of that received at the tumor and the ratio of the tumor dose to maximum skin dose is about 1.7 : 1.

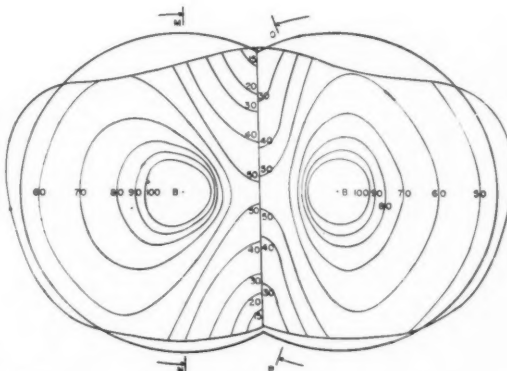


Fig. 9. Distribution on the left obtained using  $180^\circ$  rotation about both points B. Half of the resultant distribution obtained by combining these two distributions is shown on the left. The distribution on the right was obtained using  $220^\circ$  rotation in the same way. The limits of rotation are indicated. Field size  $10 \times 4$  at B, focal tumor distance 60 cm. H.V.L. 2 mm. of Cu.

If the right side of Fig. 9 is compared to the right side of Fig. 8 the advantages of the lateral  $60^\circ$  omission in Fig. 8 may be more clearly seen. The X-ray dose at the body centre is reduced from 50 to 40 per cent and the radiation received by the femoral bones is also materially reduced.



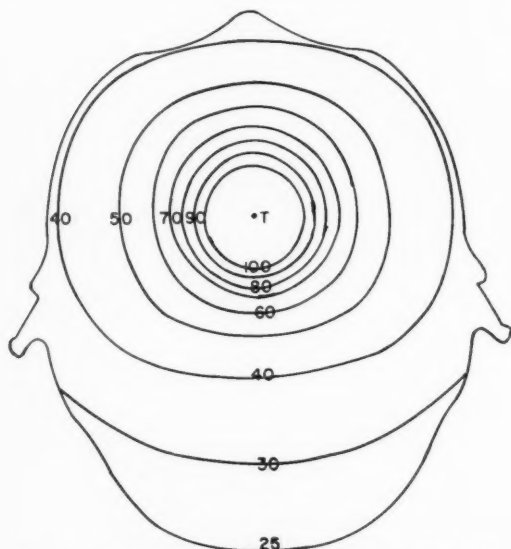


Fig. 10. Rotation distribution about a pituitary. Field size 5 x 5, focal tumor distance 60 cm., H.V.L. 2 mm. of Cu.

Figure 10 shows the distribution obtained by a 360° rotation using a field of 5 x 5 cm. in the treatment of tumors of the pituitary. Here the distributions are very regular as would be expected, and the ratio of tumor dose to maximum skin dose is approximately 2.5 : 1.

The distribution obtained using a 15 x 6 cm. field in the treatment of tumors of the mid-oesophagus is shown in Fig. 11 (left side). The tumor dose was worked out for this example in Table IV. We see that the distribution gives a tumor dose to maximum skin dose ratio of 2 : 1.

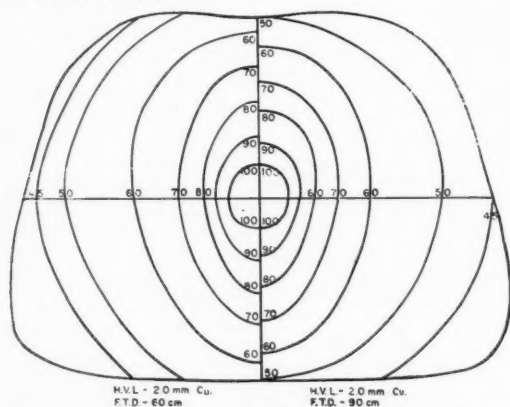


Fig. 11. Rotation distribution for cancer of the oesophagus obtained by 360° rotation about the tumor using a field size of 15 x 6 cm. H.V.L. 2 mm. of Cu.

Left side — Focal tumor distance 60 cm.

Right side — Focal tumor distance 90 cm.

### (c) Effect of Focal Tumor Distance and Quality of Radiation on Distributions

On the right hand side of Fig. 11 is given the distribution using a 15 x 6 field, H.V.L. 2.0 mm. Cu. with a focal tumor distance of 90 cm. The skin dose is now lower for the same tumor dose but the improvement is very slight and would not justify the large increase in treatment time. From this example and the discussion in the next section on "skin-air" ratios we conclude that for rotation therapy the distributions are an insensitive function of the focal tumor distance.

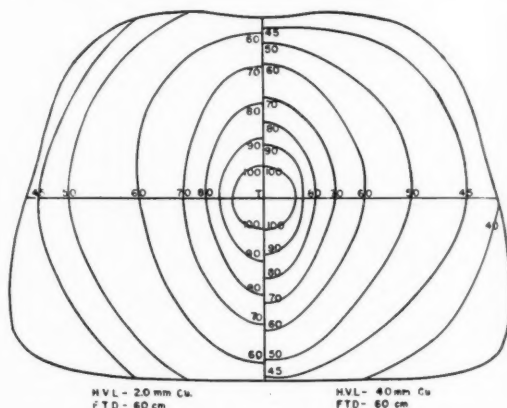


Fig. 12. Rotation distributions for cancer of the oesophagus obtained by 360° rotation about the tumor using a 15 x 6 field. Focal tumor distance 60 cm.

Left side — H.V.L. 2.0 mm. Cu.

Right side — H.V.L. 4.0 mm. Cu.

In Fig. 12 the distribution obtainable using half value layer 4.0 mm. of Cu. (right side) is compared with that using 2.0 mm. of Cu. (left side). The more penetrating radiation gives a slight improvement in tumor to skin ratio but it is doubtful whether the improvement would warrant the filtering of the beam and corresponding reduction in output. If the energy of the radiation is increased by a large amount considerable improvement in the "skin-air" ratio may be achieved.

## IV — PHYSICAL BASIS OF ROTATION THERAPY

### (a) "Tumor-Air" Ratios

In Section I the "tumor-air" ratio  $R_t$  was defined as  $\frac{D_t}{D_{ta}}$  where  $D_t$  is the dosage rate at the tumor and  $D_{ta}$  the dosage rate in air at the position of the tumor. (Fig. 1 and equation 1.) It remains to evaluate the ratio  $R_t$  in terms of known quantities, such as percentage depth

dose, backscatter, etc. From Fig. 1 we see that the dosage rate on the skin is given by

$$D_s = D_{ta} \cdot \frac{(F)^2}{(F-d)^2} (1 + b) \quad (4)$$

where  $\frac{(F)^2}{(F-d)^2}$  is the inverse square factor and

$b$  is the backscatter factor for the area of the entrance field  $A$ ,  $A$  and the area of the field at the tumor  $A_0$  are related by

$$A = A_0 \frac{(F-d)^2}{(F)^2} \quad (5)$$

Let  $P$  be the percentage depth dose for a field of area  $A$ , focal skin distance  $f = F-d$ , and depth  $d$ .  $P$  is a function of  $A$ ,  $f$  and  $d$ . The dosage rate at the tumor  $D_t$  is given by

$$D_t = D_{ta} \cdot \frac{(F)^2}{(F-d)^2} (1 + b) \frac{(P)}{(100)} \quad (6)$$

and the "tumor-air" ratio  $R_t$  by

$$R_t = \frac{(F)^2}{(F-d)^2} (1 + b) \frac{(P)}{(100)} \quad (7)$$

The expression  $R_t$  of the equation (7) is a function of  $F$ ,  $d$ ,  $b$ ,  $A$ , and can be evaluated for any combination of these parameters from the data in the depth dose survey. The method by which this may be done will be illustrated by the following example in which this ratio is determined for a field of 100 cm<sup>2</sup> at a tumor distance of 60 cm. and a H.V.L. of 2 mm. of Cu. The steps in the calculation are indicated in Table VIII.

TABLE VIII

Calculation of Tumor-Air Ratio for H.V.L.  
2.0 mm. Cu.

Focal Tumor Distance  $F = 60$  cm.;  
Tumor field size  $A_0 = 100$  cm<sup>2</sup>

(1)	(2)	(3)	(4)	(5)	(6)
DEPTH $d$	F.S.D. $f = F-d$	Area of Field $A$ (Equation 5)	Percent- age Depth Dose	Back- scatter	"Tumor- Air" Ratio
0	60	100.0	100.0	0.310	1.31
1	59	96.6	99.4	0.305	1.34
2	58	93.3	93.3	0.300	1.30
4	56	87.4	77.0	0.295	1.14
6	54	81.0	59.6	0.280	0.940
8	52	75.0	44.4	0.275	0.755
10	50	69.8	33.0	0.269	0.602
12	48	64.0	23.8	0.261	0.470
14	46	58.8	16.9	0.252	0.360
16	44	53.9	12.0	0.245	0.278
18	42	49.0	8.5	0.236	0.215
20	40	44.4	5.9	0.225	0.163

In column (1) are tabulated the depths of tissue for which calculations will be made. Column (2) is the focal skin distance which varies from 60 cm. to 40 cm. as the depth of tissue increases from 0 to 20 cm. Column (3) gives the corresponding area of field on the

skin, as determined by equation (5). Column (4) gives the per cent depth dose for depth  $d$  and surface area  $A$ , and focal skin distance  $f$ . These values are obtained from the depth dose survey through the use of suitable cross plots. The backscatter factors given in column (5) were obtained from measurements made in this laboratory. Column (6) gives the "tumor-air" ratio as calculated from equation (7). From Table VIII we see that a tumor 8 cm. below the skin surface would receive 0.755 of the dose received in air at the same point.

"Tumor-Air" ratio data obtained in this way were presented in Table I for half value layers of 1.0, 2.0 and 4.0 cm. of Cu. for a selection of circular areas. Table II contains data for rectangular fields for the same range of radiations. These tables apply to focal tumor distances from 40 to 100 cm. It should be noted that for small depths the "tumor-air" ratios are larger for the softer radiation. This is due to the larger backscatter factors for the softer radiation (see equation (7)). For large depths the "tumor-air" ratios for the harder radiations are greater because of the much greater percentage depth dose. If the "tumor-air" ratios had been expressed in terms of the output in air with full backscatter this anomaly would not have been present. The "tumor-air" ratios give one a method of calculating the dosage rate at the tumor and give no information concerning the skin dose and the skin to tumor ratio.

#### Variation with Focal Tumor Distance

The "tumor-air" ratio given by equation (7) is superficially a function of the focal tumor distance  $F$ . Detailed calculations were carried out for focal tumor distances from 50 to 100 cm. and identical results within one per cent were obtained for all values of  $F$ , indicating that the "tumor-air" ratio is independent of  $F$ . A summary of these calculations is given in Table IX.

Table IX — To Show that the "Tumor-Air" Ratio is Independent of Focal Tumor Distance  $F$ 

Calculations are for Area at Tumor  $A_0 = 100$  cm<sup>2</sup> and depth of tissue  $d = 10$  cm., H.V.L. 2.0 mm Cu.

(1)	(2)	(3)	(4)	(5)	(6)
Focal Tumor Distance $F$	$\frac{(F)^2}{(F-d)^2}$	Area of Entrance Field $A$ cm <sup>2</sup> (Equation 5)	Back- scatter Factor for Area $A$	Percent- age Depth Dose From Tables	"Tumor- Air" Ratio $R_t$ (Equation 7)
50	1.562	64.0	1.260	30.5	0.600
60	1.440	69.8	1.269	33.0	0.602
80	1.308	76.5	1.279	35.8	0.598
100	1.235	81.0	1.285	37.8	0.600

The "tumor-air" ratio  $R_t$  given in the last column is the product of columns (2), (4) and (5). As  $F$  is increased, values in column (2) decrease while those in (4) and (5) increase. The product, however, remains constant. From a physical point of view this compensation is not unreasonable. Consider Figure 1. Changing the distance  $F$  merely alters the shape of the volume of tissue which receives radiation. The ratio of the amount of primary radiation reaching  $T$  as compared with  $T_0$  depends only on the amount of overlying tissue and this is independent of  $F$ . The scattered radiation is also remarkably insensitive to changes in  $F$ . If the focal tumor distance were altered over very large limits, no doubt this conclusion would not be valid but over the limits set by our standard depth dose tables (40 to 100 cm.) this generalization is certainly valid to an accuracy of about 1%.

### Rectangular Fields

The data given in Table II for rectangular fields was obtained from the data given in Table I, using the concept of equivalent area. To find the equivalent circular area of a rectangular field, the depth dose along the central axis of the rectangle is calculated using Clarkson's method and the circular area having the same depth dose values is determined. The data of Table II was obtained from that in Table I by this method.

### Accuracy of Data

In practice the phantom surface is not a plane surface but convex one. This means that points off the axis of the beam will receive slightly more radiation than they would if a plane phantom were assumed. That is the isodose curves should be slightly flatter than they appear normally. However, as far as the axis of the beam is concerned the error made in assuming a flat surface is negligible since the dose due to primary radiation is correctly determined and the dose due to secondary radiation is an insensitive function of the depth. Tumor doses can be determined as accurately as one wishes. In Table III the radii were read off at each 20 degree interval. If greater precision were required the radii could be read off at smaller intervals. In Table III it was necessary to evaluate the tumor air ratio  $R_t$  for each radius and average. If the radius is essentially constant over the whole contour the average radius could be used to determine the average "tumor-air" ratio as in Table IV. If the "tumor-air" ratio were a linear function of the depth rather than a logarithmic one the mean radius could always

be used to obtain the average "tumor-air" ratio. If the mean radius is used the tumor dose will be underestimated slightly. The error will depend on the magnitude of the variations in the radius.

The accuracy of the tables depends upon the accuracy of the original depth dose tables and on the backscatter values used. We estimate the overall accuracy of the "tumor-air" ratio tables to be about 2%.

### (b) "Skin-Air" Ratios

The determination of "skin air" ratios  $R_s$  for circular phantoms is difficult and time consuming because of the problem of determining the dose on the skin surface due to scattered radiation. Consider Figure 4 and equation (2) of Section II (a). From equation (2) it is seen that the doses at  $P_1$  to  $P_n$  must be determined. This means complete isodose curves must be constructed. If one assumes that the skin dose is mainly produced by the entrance and exit fields large errors are made. In fact, for narrow fields such as  $15 \times 4$  the scattered radiation contributes about one-third of the total skin dose. However, the "skin air" ratio for a given field and phantom size can be obtained (by averaging the doses  $P_1$  to  $P_n$ , and comparing this dose to the output in air at the tumor position). To determine this quantity for another phantom radius a new isodose curve must be constructed for the area of the entrance field and the focal skin distance are now both different. The amount of work may be reduced somewhat by making suitable approximations and by the use of cross plots. The data presented in Table V are accurate to about 5%. One serious approximation has been made throughout in assuming that the scattered radiation in a finite circular phantom is the same as for an infinite one. Also the convex surface of the phantom will alter the scattered radiation in a complicated way which cannot be estimated. For these reasons we cannot claim great accuracy for the tables although they should be of use clinically in estimating the skin dose.

### Variation of "Skin-Air" Ratio with Focal Tumor Distance

If we consider that the entrance field produces the total skin dose the variation of "skin-air" ratio with focal tumor distance may be estimated. In Figure 13 is shown a circular phantom rotating with a period  $T$ .

Fig. 13  
dose.

The w  
to the

$W =$   
skin is

$D_s =$

backsc  
the dos  
time a

tion is  
during

$D_s (2)$

The "s

$R_s =$

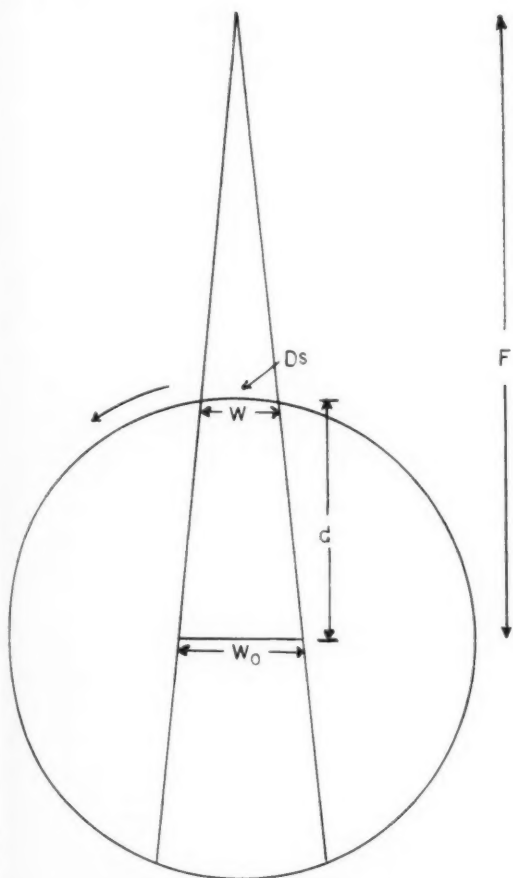


Fig. 13. Diagram illustrating calculation of skin dose.

The width of the entrance field  $W$  is related to the width of the field at the tumor by  $W = W_0 \frac{(F-d)}{F}$ . The dosage rate  $D_s$  on the skin is given by

$D_s = D_a \frac{(F)^2}{(F-d)^2} (1+b)$  where  $b$  is the backscatter for the entrance field and  $D_a$  is the dose rate in air at the tumor position. The time a point on the skin is exposed to radiation is  $\frac{(W)}{(2\pi d)}$ .  $T$ , hence the dose received during one revolution is given by

$$D_s \frac{(W)}{(2\pi d)} T = D_a T \frac{(F)(W_0)}{(F-d)(2\pi d)} (1+b)$$

The "skin-air" ratio  $R_s$  is then

$$R_s = \frac{(W_0)}{(2\pi d)} \cdot \frac{(F)}{(F-d)} (1+b) \quad (8)$$

This of course is the "skin-air" ratio for the entrance field only. In this expression  $b$  is a function of  $F$  increasing slowly as  $F$  is increased for it is determined by the size of the entrance field. If we change the focal tumor distance from  $F$  to  $F_1$  giving a new value  $R_s^1$  we have

$$\frac{R_s^1}{R_s} = \frac{(F_1)(F-d)}{(F_1-d)(F)} \cdot \frac{(1+b_1)}{(1+b)} \quad (9)$$

Consider a tumor at a depth of 10 cm. If  $F$  is increased from 60 to 90 cm. equation (9) shows that the "skin-air" ratio is reduced by

$$.937 \frac{(1+b_1)}{(1+b)}. \text{ Since } (1+b_1)/(1+b) \text{ is}$$

greater than 1.0 the actual reduction in "skin-air" ratio is less than 6%. When we take into account the fact that the scattered dose may produce 10 to 30% of the skin dose the variation with focal tumor distance will be even less than the 6%. "Skin-Air" ratios are thus a rather insensitive function of  $F$ . Detailed calculations for focal tumor distances of 60 cm. and 90 cm. bear out the above conclusions. Since "tumor-air" ratios are not a function of  $F$  the variation of tumor to skin dose with focal tumor distance will be the same as the variation of "skin-air" ratios with  $F$ . From Figure 11 we saw that the actual distributions did not depend greatly on  $F$ .

### (c) "Tumor-Skin" Ratio

In general we are interested in the ratio of tumor to skin dose. Using the approximate expression for  $R_s$  of equation (8) and the exact expression for  $R_t$  of equation (7) we obtain for the tumor to skin ratio  $R_{ts}$ .

$$R_{ts} = \frac{R_t}{R_s} = \frac{(F)(P)}{(F-d)(100)} \cdot \frac{2\pi d}{W_0} \quad (10)$$

This expression shows that for constant field size, depth and focal tumor distance the tumor-skin ratio is proportional to the percentage depth dose. In Figure 12 a distribution obtained with H.V.L. 2.0 was compared with H.V.L. 4.0. From the depth dose survey we find that for a field size of 80 cm<sup>2</sup> and depth 11 cm. focal skin distance 60 cm. the percentage depth dose increases from 30.5 to 32.0 for this change in quality. This is a 5% change. In Figure 12 we observed a 15% change in the tumor skin ratio. Expression (10) will certainly underestimate the variation of the "tumor-skin" ratio with quality since in it no account is taken of the scattered radiation. As the radiation is made more penetrating side scatter becomes less important and so the skin dose will decrease. Of course the increase in the exit dose will partially

neutralize this effect. Thus "tumor-skin" ratios are a function of quality of radiation and improvement in this ratio can be achieved by increasing the energy of the radiation. Preliminary calculations with Cobalt 60 show that for an oesophagus the tumor to skin ratio is about 3:1. This should be compared with Figure 12 which gives a ratio of 2.2:1 for H.V.L. — 4.0 and 1.8:1 for H.V.L. 2.0 mm. Cu.

### Summary

A practical method of determining the tumor doses at various sites for rotational techniques is presented using the concept of "tumor-air" ratio. Extensive tables give this ratio for a number of field sizes and for qualities of radiation in the range 1.0 to 4.0 mm. of Cu. From this data it is possible to determine the dosage rate at the tumor for rotation or partial rotation about any point in the body. Tables giving "skin-air" ratios enable one to estimate the skin dose. It is shown that rotation techniques are influenced only slightly by focal tumor distance.

Complete distributions of radiation are presented for a number of sites.

The physical justification for "tumor-air" ratios and "skin-air" ratios is described.

### Acknowledgements

*The authors wish to acknowledge the financial assistance of the National Cancer Institute of Canada.*

### BIBLIOGRAPHY

1. Nielsen, J., Jensen, H., & Thayssen, V. — *Acta Radiologica* 1944, Vol. 25, page 95.
2. Gynning, I. — *Acta Radiologica*, 1951, Vol. 35, page 428.
3. Gynning, I. — *Acta Radiologica*, 1951, Vol. 35, page 443.
4. Krebs, C., Nielsen, H. and Henderson P. E. — *Acta Radiologica* 1949, Vol. 32, Page 304.
5. Nielsen, H. — *Acta Radiologica*, 1952, Vol. 37, page 318.
6. Nielsen, J. — *Acta Radiologica*, 1945, Vol. 20, page 361.
7. Spiers, F. W. — *British Journal of Radiology*, 1946, Vol. 19, page 52.
8. Johns, H.E., Fedoruk, S.O., Kornelsen, R.O., Epp, E.R. and Darby, E.K. — *British Journal of Radiology*, 1952, Vol. 25, page 542, and *British Journal of Radiology Supplement No. 5*, 1952.
9. Love, J., Combs, G.N., Askew, W.A., Harcourt, M. — *Radiology*, 1951, Vol. 57, page 169.
10. Eycleshymer, A.C. & Schoemaker, D.M. — *A Cross Section Anatomy*, D. Appleton-Century Co. New York, 1938.
11. Clarkson, J.R. — *British Journal of Radiology*, 1941, Vol. 14, page 265.
12. Meredith, W.J. & Neary, G.J. — *British Journal of Radiology*, 1944, Vol. 17, page 126.
13. Tod, Margaret C., & Meredith, W.J. — *British Journal of Radiology* 1938, Vol. 11, page 809.
14. Meredith, W.J. — *Radium Dosage*, The Manchester System, E & S. Livingstone Ltd., Edinburgh 1947.



**THE SOLITARY PULMONARY FOCUS — CARCINOMATOUS OR OTHERWISE,  
WITH PARTICULAR REFERENCE TO HISTOPLASMOSIS.\*†**

W. A. JONES, M.D., F.R.C.P.(C), F.F.R., F.A.C.R.

Kingston General Hospital, Ontario

For a score and more years, in the district of Kingston (Ontario), we have been very curious about multiple pulmonary calcifications seen in skiagrams of the chest. Like others we had for long doubted that calcified tuberculous lesions could always account for the picture presented by these so constantly recurring findings.

On the grounds of the history of these patients, it did not seem reasonable to conclude that so many people who had never been seriously ill had in fact recovered from miliary tuberculosis. We began to think of these things as evidence of old fungus infection of some type.

After Palmer, and Christie and Peterson<sup>1</sup>, published the results of their work on Histoplasmosis in 1945 we felt that we were approaching a solution of the matter. Since then we have been able to obtain histoplasmin for skin tests, and this inference has been justified.

In Kingston we are working out the geographical distribution of our cases. Most of our patients come from the upper St. Lawrence River valley and the Bay of Quinte area but because of Queen's University we have a student population drawn from all over Canada and parts of the United States, and so our cases have a wide continental distribution.

The different acute or subacute pulmonary manifestations of the disease are of interest. We have not, in this area, so far recognized any cases in the acute phase of this disorder, and our acquaintance with such comes from other people. Dr. Clarke White of the Raybrook Sanatorium, Raybrook, New York, has been particularly helpful in this matter.

Today I want to talk about calcification seen in the lungs of these cases and more particularly about our more recent interest, the calcification of solitary foci.

If, as according to the well known Chinese proverb, one picture is worth a thousand words it would be wise to let the pictures speak. Lest I should trouble those good people who dislike the word picture, and prefer the term, radiograph, I will compromise and show you skiagrams (an older and much better name).



Figure 1

This is a common conception of histoplasmosis. Here we see the widely disseminated calcified nodules smothering the lung fields like a blizzard. Most of our cases are those of this wide-spread type of calcification.

\* Received at Editorial Office November 27, 1952.  
Publication deferred until present issue.

† Presented at Annual Meeting, Canadian Association of Radiologists, January 29th, 1953, Toronto.

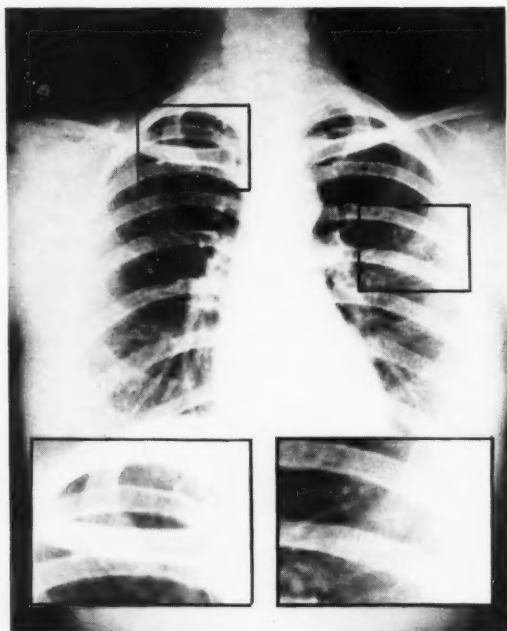


Figure 2

This is a less common form (or possibly only a less commonly recognized form). It follows pneumonic infiltration of the lung. The calcification is irregular both in form and distribution and may give little indication of the much greater extent of the original acute pneumonic lesion (Courtesy of Dr. Clarke White).

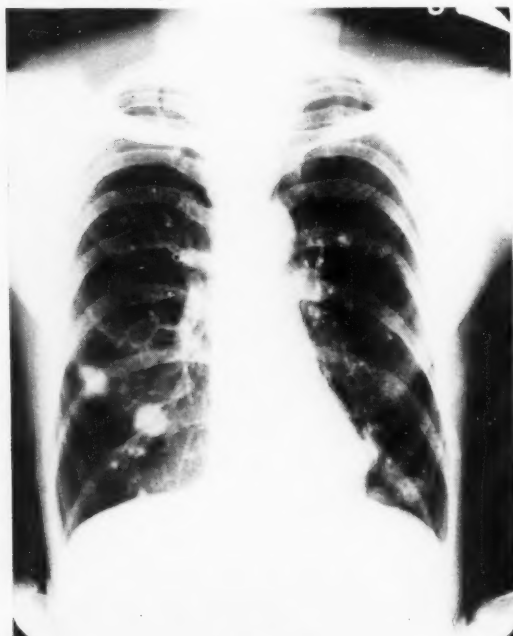


Figure 3

This is the nodular form of the disease. There are not very many nodules. Some are small. Some are quite large, measuring 2.5 cms. in diameter. Small wonder that those who first saw this film thought these nodes to be evidence of secondary carcinoma.

The calcified nucleus at the centre, however, is the give-away. This nucleus with its halo I believe to be characteristic.

This patient reacts strongly to histoplasmin. He is negative to tuberculin. The nodes have been present for several years.

This type of calcification is not as common as the widely disseminated form but it is not infrequent. The calcified nucleus may be small or fairly large. It is usually solid. The halo or aureola, is of course often found also in the widespread type of lesion but is not usually as well marked.

It is this type of lesion—the calcific centre with the aureola that is of great interest. True, tuberculous lesions may also have halos, but to my mind the presence of a solid calcified nucleus with a halo is a definite invitation to think of histoplasmosis.

If you are in a philosophic humour, you might pause to reflect upon the appearance of the nucleus with its halo. It is so similar in appearance to the Histoplasma Capsulatum, with its own capsule (or halo), that one might almost accuse nature itself of practising sympathetic magic.

I now wish briefly to deal with what to me is the main interest of this paper—the matter of Solitary Pulmonary Foci. I would like to start off by declaring the premiss upon which I base my diagnosis of such lesions when they are calcified. Realizing that other fungus infections can cause pulmonary calcification and that tuberculosis may sometimes show haloed calcification, I believe that a solid calcified nucleus with a halo, in a solitary focus, should be considered evidence of histoplasmosis unless proven otherwise.

When one hears of tuberculomas and sees the skiagrams, one wonders if all these things are in fact tuberculous.

The pathologists tell us that there is very little difference in the histology of a tuberculoma and of a histoplasmodic focus, as both are diseases causing a granulomatous reac-

tion. I  
plasmo  
culoma  
require  
examin  
diagno  
consid  
tubercu  
in these  
cases t  
as pro  
given t  
search  
out.

Now  
it as d  
invite

Solit  
as they  
usually  
culoma  
course,  
encaps  
noma,  
cysts,  
similar

How  
general  
cinoma  
today a  
not ad

Is it  
not alr  
list of  
of solit

Furc  
a num  
nodules  
a serie  
the dis  
more th

Ther  
series o  
plasmo

I pre  
help to  
and sp  
uncom

\*Since  
more, s

tion. In fact, unless one is looking for histoplasmosis, the mistaken diagnosis of tuberculoma can readily be made. Actually it is required that the specimen be stained and examined for the fungus before a definite diagnosis is possible. Let us also take into consideration, that skin tests for reaction to tuberculin are sometimes said to be unreliable in these cases. One wonders then how many cases that have been passed into the records as proven tuberculomas might have been given the label of histoplasmosis if such were searched for, and appropriate tests carried out.

Now that is my premiss. I do not accept it as dogma. Maybe it is only credulity. I invite you to investigate it.

Solitary pulmonary foci or "coin lesions" as they are often two-dimensionally termed, usually fall into the suspect group of Tuberculoma, Carcinoma and Hamartoma. It is of course, recognized that other lesions such as encapsulated pleural effusion, bronchial adenoma, lung abscess, hypernephroma, various cysts, chondroma, sarcoma, etc. may throw similar shadows.

However, the most common of all these are generally recognized to be Tuberculoma, Carcinoma and of course a good deal is written today about Hamartoma. To these three, why not add a fourth — Histoplasmosis.

Is it not curious that Histoplasmosis has not already found an established place in the list of the more commonly discussed causes of solitary pulmonary lesions?

Furcolow, Mantz and Lewis in 1947 showed a number of excellent plates of solitary nodules of histoplasmosis and state that in a series of 49 cases of the nodular type of the disease, only about one quarter showed more than one nodule.

Therefore when I now present my meagre series of three cases\* of solitary node histoplasmosis, I do it very modestly.

I present them in the hope that they will help to draw attention to this type of lesion and spur interest in something that is not uncommon in many areas of this continent

\*Since this paper was given we have found three more, smaller histoplasmodic solitary foci.

and which is probably not infrequently present in many places where it has not yet been recognized.

The three cases to be presented were radiologically diagnosed as likely cases of histoplasmosis before knowledge of skin reactions or histological findings became available. This is not considered unusual. In my opinion such a diagnosis should have first place.

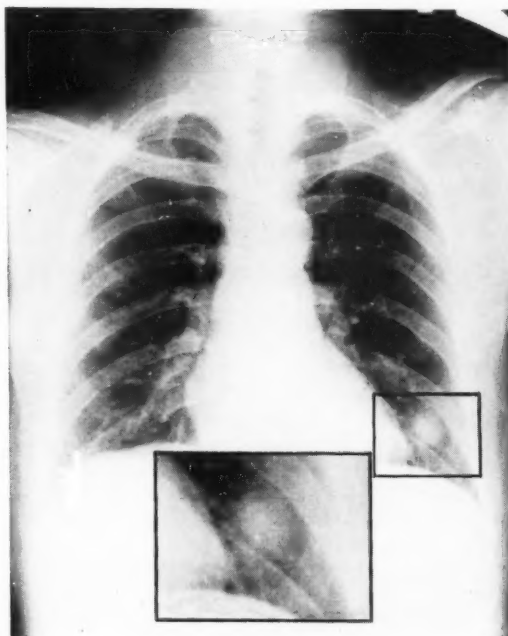


Figure 4

W.A. — male 53 years.

Respiratory symptoms negligible. Patient had a chronic cough, something that might be looked upon today as almost physiologically pathological in the cigarette smoker.

Lesion discovered in a routine film for chest examination. A solitary focus in left base with a calcified centre and a halo. Removed surgically. The section stained for fungus showed a granuloma with certain histoplasmodic characteristics. The organism *Histoplasma Capsulatum* was found in large numbers.

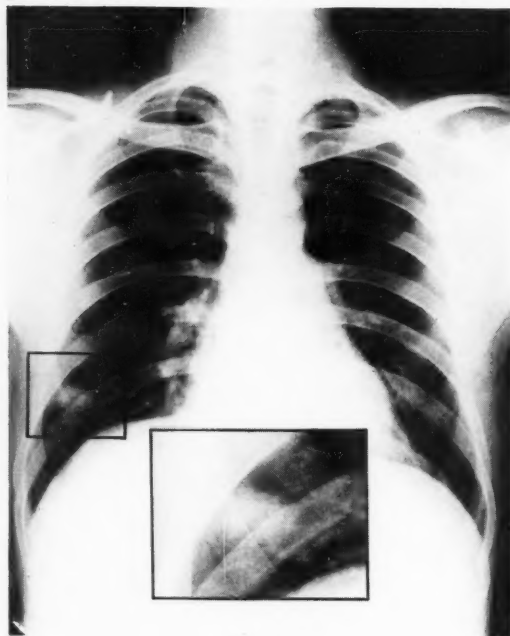


Figure 5

M.B. — male 36 years.

No respiratory symptoms. Picked up on miniature film of chest. A solitary focus in right base with a calcified centre and halo. The skin reacted strongly to histoplasmin, but was negative to tuberculin.

Section of the removed focus showed a granuloma consistent with histoplasmosis, and the organism was found.

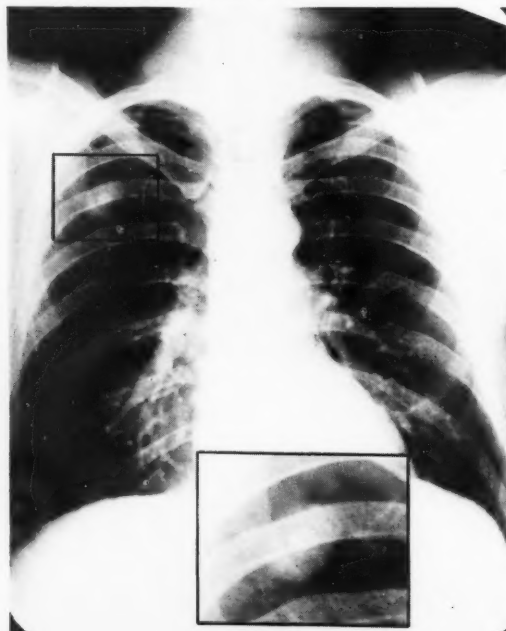


Figure 6

L.C. — male 30 years.

This shows a well developed focus with a clear cut solid nucleus surrounded by a halo. We have a series of films in this case dating back to 1940.

In 1940 the chest showed nothing unusual. In 1942 the patient had pneumonia involving the right middle lobe. At this time he first showed a small hazy focus at the site of the present lesion. We have watched this grow over the years. Both nucleus and halo become larger and more clear cut in outline year by year. This film was made in 1952. (Dr. Clarke White has shown us similar growth changes in a number of nodules in one patient).

There are no respiratory symptoms. The skin reaction to tuberculin is weakly positive while to histoplasmin it is very strongly positive. The complement fixation test for histoplasmosis is mildly positive.

In these three cases we considered chiefly the possibility of histoplasmosis, tuberculoma, carcinoma and hamartoma.

Tuberculoma was given second place because in our opinion, subject to the description that I have given, these lesions looked like Histoplasmosis — just as Niagara Falls looks like Niagara Falls. We ruled out Carcinoma on the ground of calcification. We ruled out Hamartoma on account of the type of calcification — solid instead of scattered.

In these days, when medical opinion is becoming, perhaps over-conscious of pulmonary carcinoma; when the so-called "coin lesion" has by its very name become suspect of cancer; when it is so easy to suspect a cancer of having evolved from or around an old calcified lesion of some type; it is perhaps wise to think of a simple thing, and to do a histoplasmin skin test before going on to greater things.

That last paragraph is the longest sentence in this article, and in spite of that, is probably the most important.

#### BIBLIOGRAPHY

1. Sympathetic Magic — J. G. Frazer — The Golden Bough.
2. Personal Communication — Dr. Clarke White, Raybrook Sanatorium.
3. Nontuberculous Pulmonary Calcification and Sensitivity to Histoplasmin.  
C. E. Palmer — Pub Health Rep 60:513-520 May 45.
4. Pulmonary Calcification in Negative Reactors to Tuberculin.  
A. Christie and J. C. Peterson Am. J. Pub. Health 35:1131-1147 Nov. 45.

5. The Roentgenographic Appearance of Persistent Pulmonary Infiltrates Associated with Sensitivity to Histoplasmin. M. L. Furcolow, H. L. Mantz and I. Lewis — Pub Health Rep 62:1711-1718 Dec. 47.

6. Exploratory Thoracotomy in Management of Intrathoracic Disease J. B. Grow, M. L. Bradford and H. W. Mahon — Thoracic Surg. 17:480 - 494 Aug. 48.

7. Studies of Pulmonary Findings and Antigen Sensitivity Among Student Nurses.

L. B. Edwards, I. Lewis and C. E. Palmer — Pub Health Rep 63:1569-1591 Dec. 48.

8. Surgical Treatment of Round Tuberculous Pulmonary Lesions (Tuberculomas). H. W. Mahon and J. H. Forsee — J. Thoracic Surg 19:724-740 Apr. 50.

9. Clinical and Pathological Aspects of Tuberculosis of Lung. H. Black and L. V. Ackerman — S. Clinic. North America 30:1279 - 1297 Oct. 50.

10. Hamartoma of Lung: Improbability of Pre-operative Diagnosis. W. E. Lemon and C. A. Good, — Radiology 55:692-699 Nov. 50.

11. Significance of Solitary Pulmonary Tumors. E. W. Davis and R. G. Klepser — Clin. North America 30:1707-1715 Dec. 50.

12. Isolation of Histoplasma Capsulatum from Soil. L. D. Zeidberg, L. Ajello, A. Dillon, and L. C. Runyon. Amer. Jour. of Pub. Health. — 42:930-935 Aug. 52.

13. Comparison of Histoplasmin Sensitivity Rates Among Human Beings and Animals in Boone County, Missouri. Amer. Jour. of Pub. Health — M. L. Furcolow and R. W. Menges 42:926-929 Aug. 52.

*I wish to thank Dr. Clarke White, Dr. W. H. Hay, Dr. G. F. Kipkie, Dr. J. H. Orr and others for their help in preparing this paper. I wish also to thank Mr. Philip Mott for his kindness in preparing the reproductions used in this paper.*

## POSITIONS AVAILABLE

"Radiologists — Applications for immediate radiologist appointments are invited by the Vancouver General Hospital. Please apply, stating training and experience, to the Director, Department of Radiology, Vancouver General Hospital."



## THE MEASUREMENT OF RADIOACTIVE IODINE IN VIVO

L. G. STEPHENS-NEWSHAM, Ph.D.

Department of Radiology, Royal Victoria Hospital  
Montreal, Canada

## Introduction

Iodine 131 of 8.0 day half-life decays in a complex fashion with the emission of four beta-ray groups having a maximum energy of 812 kev.<sup>2</sup> 80% of these disintegrations are followed by a 364 kev gamma-ray with weaker components of 9.3% 637 kev, 5.3% 284 kev, 2.17% 80 kev and 2.8% 722 kev. Since the maximum range of the beta particles in tissue is only 2.8 mm. they cannot be detected outside the body unless they originate in the skin. The gamma radiation, however, is only partially absorbed, having a half-value layer of about 23 cm. in tissue. Since radioactive iodine is highly localized in the thyroid it may be detected easily in vivo by some gamma-sensitive instrument and even assayed. If a directional type of detector with a small aperture is used its distribution in the gland may be "mapped". This assay of radioiodine uptake and "mapping" are useful aids to diagnosis of thyroid disease.

All Geiger counters will detect gamma photons but their efficiency is low (around 1%) compared to that for beta detection. Their efficiency, particularly for soft gammas, may be increased considerably by constructing the counter cathode of material of high atomic number.<sup>(3)</sup> Thus a lead-walled counter is about 6 times as efficient as a brass one for iodine-131 gammas. The recent development of scintillation counters has resulted in a very highly efficient gamma detector which responds to about 60% of the incident iodine-131 gammas.<sup>1</sup> The electronic requirements for these devices are more complicated and they are rather fragile.

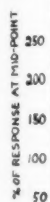
For a point source of radiation the counting rate will fall off inversely as the square of the distance. Thus if a given counter is calibrated with a known source and then used to measure the amount of radioactivity in the thyroid the exact distance to the thyroid must be known, a factor often difficult to ascertain. In practice, it is necessary to measure the counting rate at several distances and then to plot the reciprocal of the square root of the counting rate against the distance from the neck. The intercept on the distance axis will give the thyroid position.<sup>5, 7, 8</sup> Moreover, the thyroid does not behave as a point source unless large distances are used so that the counting rate is low.

Several workers have suggested multiple counter arrangements with two to four counters arranged around the neck.<sup>6, 9</sup> The efficiency is high and the counting rate is fairly independent of position since the farther the thyroid is from one counter the nearer it is to another. Thus, once calibrated, only one measurement need be made for each determination. The disadvantage is that the patient must be in a sitting position and it is difficult to get a thigh background count. Freedberg<sup>6</sup> used four platinum counters in a 50 cm. circle and found the counting rate constant within -5% in a 10 cm. circle. The efficiency was low, giving only 21 counts per minute per microcurie. Tait,<sup>9</sup> using two lead counters, found a similar latitude of motion of the source and the efficiency was 375 counts per minute per microcurie.

Gamma-rays are absorbed and scattered, which alters the counting rate when the source is inside tissue. Scattered radiation is softer and more easily detected by lead counters, so that these detectors will record an increased counting rate even though the absorption tends to reduce it. Many workers have calibrated their counters with the source inside a phantom simulating the neck or in a cadaver. In general the counting rate is increased when the source is inside the neck, 8 to 15% being reported as the amount of increase. It might be expected that this will vary, depending on the size of the scattering material and the amount of tissue between counter and source, as well as on the type of counter.

## Design of a Counter for Total Uptake Measurement

A two counter arrangement was considered best, since the tubes must be operated at the same voltage and more than two become difficult to match. The counters were G10Pb lead-walled counters (designed by the British Medical Research Council). These were mounted in  $\frac{3}{4}$  inch lead shields having apertures 3.8 by 10 cm. as shown in Figure 1 and supported on an old X-ray tube stand with a spacing of 40 cm. between centers. With this arrangement the counters could be placed with one behind and one in front of the neck of the patient either sitting or lying in bed. Also a background on the thigh could be taken.



A 1 curies axes the counter being counting a variety all side tancy above The gave 1 air, the 1 micro with a count.



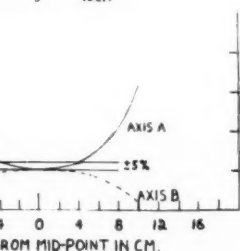
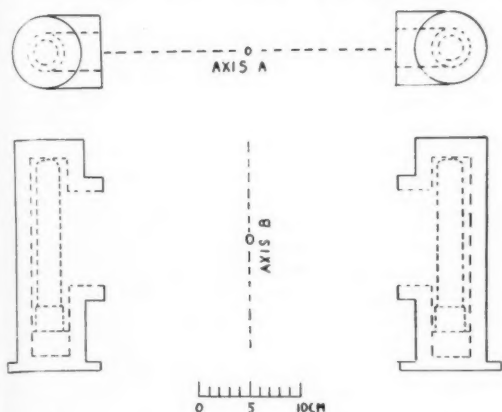


Figure 1

A 1 cc. sample containing about 20 microcuries of radioiodine was moved along the two axes through the mid-point between the two counters, the variation of the counting rate being shown in Figure 1. It is seen that the counting rate was constant within  $\pm 5\%$  for a variation of source position of 4 cm. on all sides of the mid-point. A similar constancy for a vertical displacement of 2 cm. above and below was found.

The two counters, connected in parallel, gave 188 c.p.m. per microcurie for a source in air, the background being 90 c.p.m. Thus only 1 microcurie in the thyroid could be detected with a statistical accuracy of 5% in a 3 minute count.

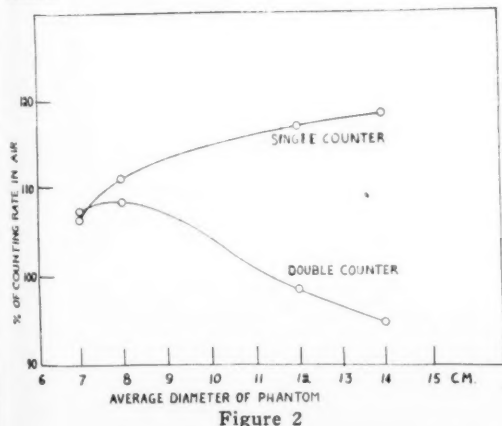


Figure 2

### Backscatter and Absorption

Slightly elliptical hollow cylinders of various diameters were constructed of washed X-ray film and filled with water. The cylinders were adjusted between the counters in the position of a neck so that a small radioactive source, central to the two counters, was 2 cm. from one face of the cylinder. Figure 2 shows the variation of counting rate with phantom diameter compared to that without the phantom, using both counters and then only the one farthest from the phantom. The latter counter has a constant amount of absorber between it and the source and the backscatter is seen to increase the counting rate up to a maximum of about 16%. Using two counters, the other one has increasing amounts of absorber in its way so that the overall counting rate decreases.

A hollow plastic model of the neck was moulded from a plaster cast and filled with water, cervical vertebrae being added. On inserting a small radioactive source at the level of the thyroid, the counting rate increase was 8% over that in air. Consequently this figure has been used to correct all readings of iodine in the thyroid, since the counters are calibrated by the counting rate of the source in air. The counting rate was substantially constant for all possible positions of the source inside this phantom.

Figure 3 shows a typical uptake curve measured on a patient. The curve is seen to be smooth, and satisfactory agreement between the amount taken up, the amount excreted and the dose given has been found.

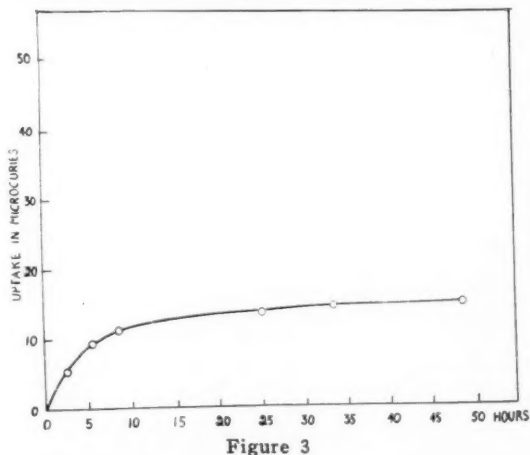


Figure 3

### A Directional Counter

Veall<sup>10</sup> and Corbett and Honour<sup>4</sup> have described counters for directional work consisting of a long narrow geiger counter in a lead

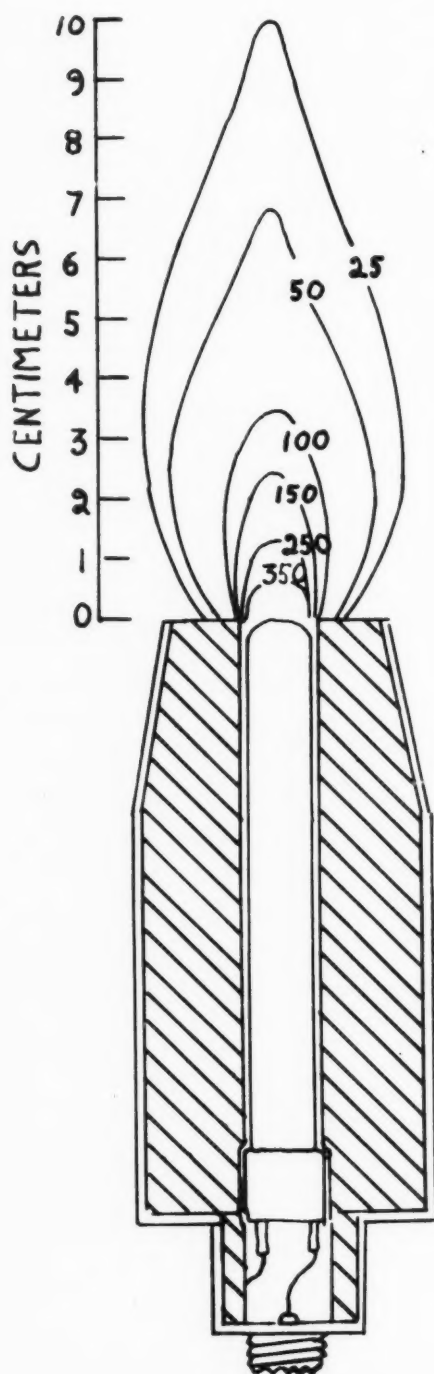


Figure 4

shield with an annular opening at one end. Such a counter responds to only a narrow pencil of rays and can be used to delineate the thyroid after it has taken up radioiodine. A modification of this counter has been designed. A G4Pb lead counter tube, whose diameter is  $\frac{1}{2}$  inch, was enclosed in a  $\frac{1}{2}$  inch lead shield with an opening at one end. Figure 4 shows the variation of counting rate around the nozzle of this counter for a small source, expressed in counts per 50 sec. per microcurie. Though not so directional as Veall's counter, it was more sensitive and the presence of nodules could readily be detected. The thyroid could be outlined after only two hours from the administration of a 50 microcurie dose.

### Summary

The problem of measuring the amount of radioiodine in the thyroid by external gamma counting has been discussed.

A double counter arrangement for measuring total uptake has been described, permitting the amount of radioiodine in the thyroid to be measured with an accuracy of  $\pm 5\%$  without knowing the exact position of the thyroid.

The correction necessary for backscatter and absorption was determined and found to be variable with the size of the neck. For a single counter it has been found to have a maximum of 16% and for a double counter it was about 8% for average sizes of necks.

A directional counter has been described which permits the thyroid to be outlined with a dose of only 50 microcuries but which has a sufficiently sharply defined aperture to permit single nodules to be located.

### REFERENCES

1. Allen, H. C. and Goodwin, W. E. *Radiology*, 1952, 58:68-74.
2. Bell, R. E. and Graham, R. L. *Phys. Rev.*, 1952, 86:212-218.
3. Bradt, H. et al. *Helvetica Phys. Acta*, 1946, 19:77.
4. Corbett, B. D. and Honour, A. J. *Nucleonics*, 1951, 9:43.
5. Fields, T. and LeRoy, G. V. *Radiology*, 1952, 58:57-67.
6. Freedberg, A. S. *J. Clin. Endocrin.*, 1950, 10:910.
7. Myant, N. B., Honour, A. J. and Pochin, E. C. *Clin. Sci.*, 1949, 8:135.
8. Oddie, T. H. and Scott, R. K. *B.J.R.*, 1949, 22:698-705.
9. Tait, J. F. et al. *B.J.R.*, 1951, 24:14-16.
10. Veall, N. *B.J.R.*, 1950, 23:527-529.

## GASTRIC DIVERTICULA

K. E. MATZINGER, M.D.

General Hospital - Ottawa

Compared with the frequency of diverticulosis in other parts of the gastro-intestinal tract, diverticula of the stomach are rare. Palmer<sup>1</sup> on reviewing the literature found 412 cases reported. Their incidence based on routine roentgen examinations of the stomach varies in different reports. Fels and Simril<sup>2</sup> found 31 cases of gastric diverticula diagnosed from about 30,000 barium studies, which gives an incidence of about 0.10 per cent. Rivers, Stevens and Kirklin reported 25 diverticula from 90,000 examinations, an incidence of 0.03 per cent; and Palmer,<sup>1</sup> reviewing reports by a number of authors, found the diagnosis made in 165 from 380,099 G.I. series, an incidence of 0.043 per cent.

A wide variety of etiological factors is cited. The true diverticula, which are outpouchings of all layers of the gastric wall are probably of congenital origin. Their predilection for the infracardiac region of the stomach and the posterior wall where 76% were found, and their occasional discovery in infants and young children (10 of 267 diverticula were found in the first 10 years of life according to Palmer) would favor this etiology. In 12 of 90 Palmer's cases, where a pathologic examination was carried out, the diverticulum was found to contain aberrant pancreatic tissue. These diverticula were located in the prepyloric and pyloric region, where aberrant pancreatic nests are not uncommon. Aberrant pancreatic tissue in the prepyloric region, visible microscopically, has according to Littner and Kirsh,<sup>4</sup> a typical radiological appearance. A round filling defect with a central depression in the shape of a crater from 0.6 cm. to 1 cm. in depth was present in 6 of their 7 cases. These findings would favor the congenital etiology of the two anomalies, the diverticulum being secondary to the aberrant pancreatic tissue.

On the other side, diverticula caused by other gastric pathology, classified as false diverticula, can be due to a wide variety of causes, such as perigastric adhesions, gastritis, syphilis of the stomach, increased intragastric pressure, foreign bodies in the stomach (coins-Kaufman<sup>3</sup>), penetrating gastric ulcers with circumscribed perforation, adhesions secondary to gastric ulcers, outpouching of the ulcerated area which constitutes a locus minoris resistentiae, scar formation after ulceration with retraction and

formation of a diverticulum—like pouch, and ulcerating benign tumors, most frequently neurofibromas (Schwannomas). The secondary diverticula were not included in the reported cases.

The symptomatology in uncomplicated cases was pain in the lower chest and epigastrium worse after meals, dyspepsia, eructations, pyrosis, flatulence and fullness after meals.

The diagnosis is made as a rule by a barium meal. The diverticulum in some cases fails to fill, due to spasm of its neck. This, according to Palmer, occurred in 14 of 262 cases during the first examination and in 6 of these even repeated barium studies failed to reveal the diverticulum which was known to be present.

Gastroscopy appears to be quite safe although less reliable.

Gastric diverticula are a rather harmless condition and complications are rare. Acute perforation occurred in 3, and massive hematemesis in 3 of 144 cases (Palmer), an incidence of about 4%. Of importance is the frequency of associated gastro-intestinal pathology. Cholelithiasis, gastric and duodenal ulcer and diverticulosis of the colon were the most frequent conditions found in these patients and accounted for the symptoms in over half of the cases. This is a warning for the radiologist to rule out other gastro-intestinal disease before satisfying himself that the diverticulum is the cause of the patient's symptoms.

Treatment in cases where the severity of symptoms warranted operation, was simple amputation of the diverticulum, more rarely invagination or partial gastrectomy. The majority of uncomplicated cases does not seem to require operation. It is of interest to note that of 131 cases operated upon, in 8 the surgeon was unable to find the diverticulum.

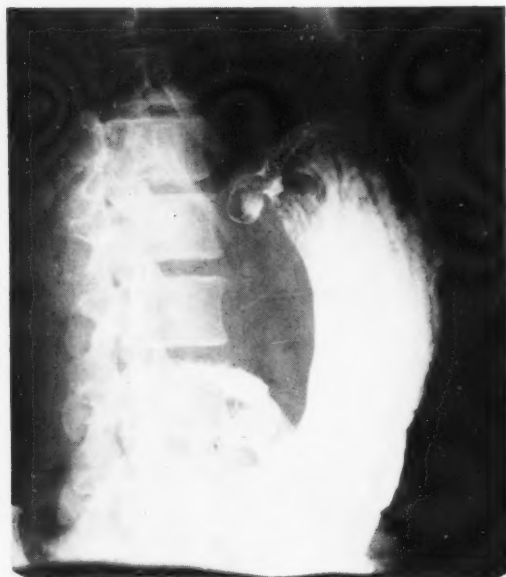
The radiological examination of a true diverticulum shows a sac-like outpouching of the gastric mucosa, with intact mucosal rugae at the neck of the sac. There is no tenderness on palpation. A retention of barium for 24 hours and longer is observed. A layer of fluid



and air can be sometimes seen on top of the barium. A cascade stomach can easily be confused with a broad shallow diverticulum of the infracardiac region. Here oblique projections, the persistence of the deformity in the supine and prone positions and retention of barium in the sac after 6 and 24 hours help to differentiate the two. A gastric ulcer can be distinguished by the history, the convergence of the mucosal folds and the decrease in size after treatment. In doubtful cases, gastroscopy helps to confirm the diagnosis.

#### Report of two cases:-

The first is a 39 year-old female, who was referred to the Ottawa General Hospital from the Hotel Dieu Hospital of Cornwall, Ontario, for operative treatment, with the diagnosis of a diverticulum of the stomach. Her history revealed the following: She complained of eructations and flatulence after every meal for the past 3 years. She suffered from bilateral sciatica for the past 8 years, and also complained of general weakness and tiredness.



Case 1

The physical examination was negative. A barium meal revealed a diverticulum at the typical location below the cardia at the posterior wall close to the lesser curvature. Twenty-four hour retention in the diverticulum was observed. On exploration no diverticulum was found in spite of a careful search.

On inquiring from the patient a year after the exploration we learned that a marked improvement had taken place with only occasional burning in the epigastrium.



Case 2

The second case was referred to the Ottawa General Hospital with the diagnosis of gastric diverticulum made on a previous barium study done at St. Michael's Hospital in Buckingham, P.Q.

This patient, a 51 year-old farmer, complained of epigastric pain for the past 15 years, worse for the past 4 months. One hour after eating, he felt discomfort in the epigastrium, accompanied by belching. Drinking water gave relief. The discomfort usually subsided after two or three hours. The barium meal revealed a diverticulum measuring 3 x 3.5 cms located below the cardia on the anterior wall. Retention of barium in the diverticulum after six hours was present. The remainder of the examination was unremarkable. The gastroscopist reported a diverticulum of 1 cm. diameter on the anterior part of the stomach close to the cardia. No signs of gastritis or ulcer were seen. The patient was explored, but no diverticulum was found. An unusual laxity of the oesophageal hiatus of the diaphragm was thought to be the cause



of the patient's symptoms and this was corrected. On re-examination two months after the operation the radiological appearance was unchanged, i.e. the diverticulum was present as before. The patient's symptoms have remained the same as prior to the operation.

#### Summary:

A short description of two cases of gastric diverticula together with roentgen findings, and the gastroscopic findings in one of these is given.

#### BIBLIOGRAPHY

1. Palmer, E. D. Gastric Diverticula, Surgery, Gynecology and Obstetrics, 1951, 92: 417 - 428.
2. Fels, R. W. and Simril W. A. Gastric Diverticula, Amer J. Roentgenol. 1952, 68:8 - 14.
3. Kaufmann:— Spec. Path. Anatomie Vol. 1 9th and 10th Ed. 1931, W. de Gruyter, Berlin.
4. Littner, M. and Kirsh J. Aberrant pancreatic tissue in the gastric antrum, Radiology, 1952, 59: 201 - 210.

### SPECIAL GENERAL MEETING — JUNE 1953

#### Winnipeg, Manitoba

The Special General Meeting of the Canadian Association of Radiologists will be held in Winnipeg, Manitoba, in conjunction with the Annual Convention of the Canadian Medical Association, as follows:

Meeting of Council 2 P.M. Tuesday, June 16th, 1953  
 Special General Meeting and Dinner: 7 P.M. Tuesday, June 16th, 1953.  
 Both sessions will be held at the Royal Alexandra Hotel.

NOTE: If there is any change in the foregoing, you will be advised by special bulletin.

## In Memoriam

It is with deep regret that the Canadian Association of Radiologists records the deaths of two member radiologists during the year 1952.

BERNSTEIN, Arnold

1898, Germany.

M.D. — Albertus University, Germany, 1922.

PATERSON, R. K.

September 23rd, 1878, Greenock, Scotland.

M.D. — Queens University 1906.

## STUDY VISITS — FRANCE

In order to facilitate the stay of foreign Congress Members in France — before going to Copenhagen, the FRENCH ELECTRO-RADIOLOGY SOCIETY and its AFFILIATES are organizing study visits in Paris and the Provinces from July 6th to 17th 1953, which will include visits to the *Electro-Radiology Services* and *Anti-Cancer Centers*, as well as accounts of any new or special techniques, practical demonstrations, etc.

To participate in these "Study visits", please apply to ANTOINE BECLERE CENTER indicating your preferences as to: subjects (diagnosis or therapy); town, dates, language, etc.

## BOOK REVIEW

### THE SKULL AND BRAIN: ROENTGENOLOGICALLY CONSIDERED

C. WADSWORTH SCHWARTZ, Ph.B., M.D., F.A.C.R.

LOIS COWAN COLLINS, B.S., M.D.

Charles C. Thomas, 1951

The authors state "We have merely gathered together illustrations of the conditions which we have found to occur most frequently and have added a few examples of the rare types of pathology . . ." The 365 illustrations are well chosen for this purpose but the reproductions of the radiographs are not up to journal quality, certainly poorer than one expects in an atlas of skull radiographs. It is also disappointing that the tables and illustrations often do not accompany the text.

The chapters on the normal skull and the variants of normal are short and marred by the occasional incorrect use of terms. The chapter on lesions of blood vessel origin makes little mention of recent advances in cerebral arteriography. Figure 195 is

upside-down. It is disappointing to learn that the authors believe that the displacement of the pineal gland shows only the hemisphere in which the tumour is situated.

There are three useful charts summarizing the characteristics of lesions close to the sella turcica, of cerebral tumours in general, and of the gliomata in particular.

This little book actually contains a wealth of information. However, it is put down in a rather casual way so that it may not be considered at its true worth. It does fulfil its purpose of being a ready reference for those who may be called upon to examine skull radiographs.

D. L. McRAE

## EDITORIAL

### "LA RADIOLOGIE À LA CROISÉE DES CHEMINS"

Pour ne pas s'égarer au carrefour où elle se trouve actuellement, la Radiologie Canadienne doit chercher avec circonspection la voie qui la conduira à son complet développement et permettra à ses adeptes de rayonner dans leurs milieux médicaux respectifs.

D'abord confiné à l'examen du squelette et des poumons, le Radiodiagnostic s'est étendu à presque tous les organes du corps humain. Aujourd'hui, toutes les branches de la Médecine recourent à lui pour découvrir, localiser ou délimiter une lésion.

Les connaissances requises pour satisfaire aux exigences du Radiodiagnostic moderne, sont devenues très vastes. Aussi, le même radiologiste pourra-t-il continuer à embrasser avec compétence toutes les particularités du radiodiagnostic adaptées aux diverses disciplines médicales, ou devra-t-il partager cet immense domaine avec un ou plusieurs autres confrères.

Si un radiologiste désire avoir une connaissance générale des spécialités auxquelles il apportera sa collaboration, devra-t-il consacrer plus de quatre années à sa formation et attendre de bien maîtriser toutes les techniques spéciales du radiodiagnostic avant de prendre la direction d'un service de Radiologie ? Et s'il ne désire pas explorer toutes les avenues du Radiodiagnostic, pourra-t-il être admis aux examens du Certificat de spécialiste en Radiologie diagnostique et aura-t-il droit d'être mis sur le même pied que celui qui a étudié toutes les techniques différentes de la Radiologie diagnostique ?

Médecins et Chirugiens, demandent à la Radiologie des renseignements de plus en plus précis et exigent d'elle des diagnostics de plus en plus exacts. Les améliorations de l'appareillage radiologique fourniront-elles au Radiodiagnostic les moyens de répondre à ces desiderata et les radiologistes devront-ils approfondir davantage leurs connaissances anatomiques, physiologiques et pathologiques pour parvenir à faire des diagnostics plus rigoureux. Voilà mes chers collègues, un sujet de réflexion qui ne manque ni d'ampleur, ni d'opportunité. Lorsque vous l'aurez médité longuement, peut-être arriverez-vous à la même conclusion que moi : A l'avenir, les Radiologistes devront recevoir une formation de plus en plus profonde et de plus en plus étendue pour remplir le rôle qu'attendent d'eux médecins et chirurgiens.

Lorsque vous aurez fait un tour d'horizon sur le Radiodiagnostic, je vous invite à en faire un autre sur la Radiothérapie. Cette nouvelle discipline de l'art de guérir a pris, en ces dernières années, une expansion considérable. Les multiples recherches entreprises sur les effets biologiques des Radiations et les nombreuses observations des résultats cliniques obtenus avec les Radiations, ont élargi considérablement le champ de la Radiothérapie. Les lésions inflammatoires, les troubles fonctionnels et les processus tumoraux bénéficient de plus en plus de la Radiothérapie, depuis qu'une répartition plus judicieuse des doses dans le temps et dans l'espace, permet d'obtenir des effets thérapeutiques mieux appropriés aux diverses affections.

Où s'arrêteront les progrès de la Radiothérapie ? Nous ne le savons pas. Mais ce que nous savons, c'est que pour les suivre de près, un radiologiste devra leur consacrer tout son temps et tous ses efforts. Alors se pose la question suivante : "Est-ce que le futur radiologiste continuera à étudier à la fois le radiodiagnostic et la Radiothérapie ou bien est-ce qu'il ne s'adonnera qu'à l'étude de l'une ou de l'autre de ces deux disciplines radiologiques, tout à fait différentes". La connaissance approfondie des bases physiques et biologiques de la Radiothérapie, l'étude détaillée des techniques radiothérapiques et les observations minutieuses des réactions biologiques et cliniques que provoquent les radiations, n'ont rien de commun avec les bases, les techniques et les résultats du Radiodiagnostic.

Vous savez tous, mes chers confrères, que les radiations émises par les éléments radioactifs artificiels tels les Radioisotopes, ont les mêmes effets thérapeutiques que celles émises par les éléments radioactifs naturels tels le Radium et le Mésotorium et, que celles émises par les ampoules à R.X.

Les radiothérapeutes de demain devront-ils se préparer à l'usage thérapeutique de toutes les modalités des radiations ou pourront-ils opter pour l'une ou l'autre des diverses formes de radiations ? Et dans ce dernier cas comment subdivisera-t-on la Radiothérapie ? En deux branches ? La Radiothérapie externe, comprenant les Rayons X, le Radium et la Bombe de Cobalt 60, en applications externes ou intra-cavitaire et la Radiothérapie interne, comprenant les Radioisotopes et tous les autres éléments radioactifs utilisés en ingestion ou en injection ? Ou bien en trois branches ? la Radio-

thérapie à super voltages, la radiothérapie à voltages modérés et la Radiothérapie avec les substances radioactives.

Le radiothérapeute qui désirera couvrir tout le champ de la Radiothérapie: Roentgenthérapie ordinaire et à super voltages, Curiothérapie de surface et intra-cavitaire, Radioisotopothérapie externe et interne, devra-t-il consacrer plus de deux ans à l'étude de sa spécialité? Et celui qui désirera ne pratiquer qu'une partie de la Radiothérapie, devra-t-il subir quand même les examens sur toutes les modalités de la Radiothérapie pour être reconnu par le Collège Royal comme spécialiste en Radiothérapie? Toutes ces questions mériteraient, il me semble, d'être discutées à nos réunions annuelles. Et les résolutions dont elles feraient l'objet, pourraient ensuite être adressées aux associations médicales ainsi qu'aux administrations hospitalières qui en profiteraient sûrement. Elles doivent suivre la marche du progrès de la Radiologie si elles ne veulent pas se trouver un jour dans une impasse.

Messieurs, s'il est opportun que nous méditions sur les problèmes suscités par le développement rapide de la Radiologie, il n'est pas moins opportun que nous méditions sur nos Relations avec les administrateurs d'hôpitaux, avec les médecins et les chirurgiens, ainsi qu'avec les directeurs des plans médicaux prépayés. Car, de notre attitude actuelle sur ces questions, dépendra le sort des futurs radiologistes.

Les administrateurs d'hôpitaux ont tendance à considérer les Radiologistes comme des techniciens et à leur payer des salaires fixes, comme ils font pour leurs employés. Ces administrateurs semblent oublier que nous sommes des médecins à qui les malades se confient pour examen ou pour traitement. Notre dignité de médecins exige que nous réagissions contre la fausse conception que les administrateurs ont des radiologistes. De plus, les chefs des services de Radiologie devraient exiger des administrateurs le privilège de pouvoir choisir leurs assistants, leur personnel technique, leur appareillage et tout leur matériel de travail, puisqu'on les tient responsables du bon fonctionnement et du rendement de leurs services.

Les médecins qui s'adressent au radiologiste pour établir, confirmer ou préciser leur diagnostic devraient être assez logiques pour lui reconnaître

le titre de consultant. De même, les chirurgiens devraient accorder au radiologiste qu'ils appellent à leur secours, le titre de consultant. Pourquoi les radiologistes qui examinent des malades ou les traitent, à l'instar des médecins et des chirurgiens, ne seraient-il pas mis sur le même pied qu'eux? Serait-ce parce que leurs techniques d'examen ou de traitement sont très différentes de celles des médecins et des chirurgiens? Pourtant! les différences de techniques utilisées par les médecins et par les chirurgiens ne les empêchent pas de se considérer respectivement comme des consultants. Bien au contraire! D'ailleurs, c'est parce que leurs techniques sont différentes qu'ils ont besoin les uns des autres. Radiologistes! il importe de faire reconnaître dès maintenant, par nos confrères médecins et chirurgiens, le titre de consultants qui nous revient de droit. Demain, il sera trop tard!

Les plans médicaux prépayés n'accordent aucune rétribution au radiothérapeute qui traite une maladie de Hodgkin ou un cancer du col utérin, ou un lymphosarcome; mais ils rétribuent le chirurgien qui traite les mêmes affections. Cette partialité des Compagnies d'Assurance ne force-t-elle pas le patient, qui désire bénéficier de son assurance, à subir un traitement chirurgical plutôt qu'un traitement radiothérapique, même lorsque le traitement chirurgical s'avère moins efficace que le traitement radiothérapique. C'est une injustice envers les radiothérapeutes qui ne reçoivent aucune rémunération pour le traitement des malades qui paient des primes d'assurance aux compagnies sus-mentionnées et, un manque d'équité envers les assurés qui ont un droit strict au meilleur traitement, même si ce traitement est la Radiothérapie. Le refus inexplicable de certaines compagnies d'assurance de défrayer une partie du coût des traitements radiothérapiques de leurs assurés, devrait être signalé aux patients qui viennent nous consulter pour ces traitements.

Mes chers collègues! la Radiologie Canadienne est à un tournant de son histoire. C'est de nous Radiologistes de 1953 que dépend son avenir brillant ou terne. Arrêtons-nous donc un moment et donnons-nous la peine de regarder attentivement autour de nous pour bien choisir la voie où nous engagerons la Radiologie. Car, ne l'oublions pas, la Radiologie est actuellement à la Croisée des Chemins.

ORIGÈNE DUFRESNE, M.D.



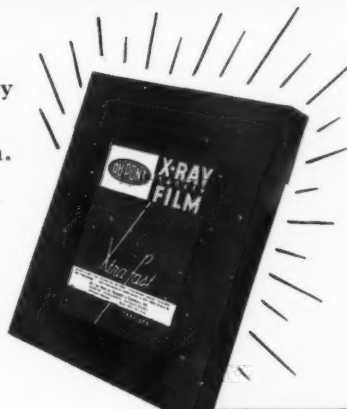


*you'll obtain roentgenograms  
of superior diagnostic contrast with*

**Du Pont**  
X-RAY FILM

The interpretive value and uniformity of roentgenograms made with Du Pont X-ray Safety Film explain why more and more radiologists and their technicians highly endorse this fine film.

Du Pont "Xtra-Fast" X-ray Film—Type 508—produces roentgenograms that clearly reveal pathological conditions of bone and tissue. The film has a blue safety base that further enhances the image. Try it for roentgenograms of superior diagnostic contrast.



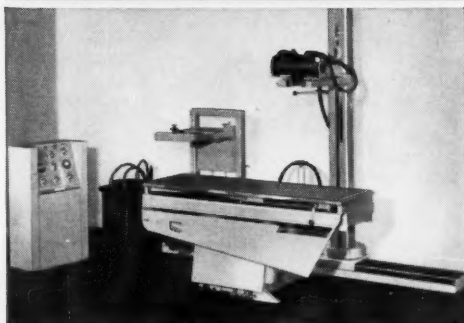
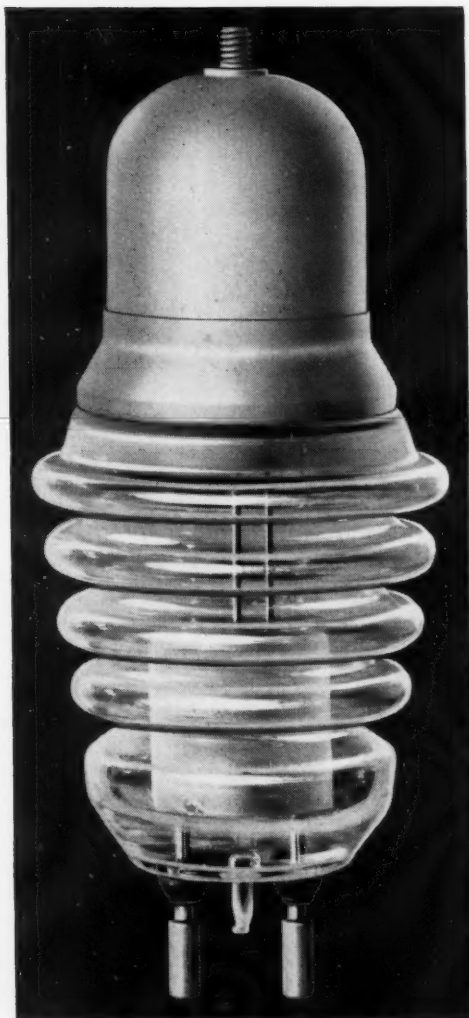
**CANADIAN INDUSTRIES LIMITED**  
MONTREAL



PP53-2

SERVING CANADIANS  
THROUGH CHEMISTRY

# How often do YOU replace valve tubes?



This Maxicon 200, like all valve-rectified GE x-ray units, uses long-life GE kenotrons.

If it's every few months—  
or even every few years  
—here are facts about  
GE kenotrons that can  
mean big savings for you

REPORT OF KENOTRON LIFE  
ON 83 GE X-RAY UNITS

Group* (from 4 geographic areas)	No. of x-ray units	Average years of service	Total kenotrons involved	No. of valves replaced
A	6	6	24	1
B	18	15	72	8
C	53	8	212	4
D	6	10	24	2

\*Names supplied on request

At General Electric, quality is more than an abstract word. It's actually built into every component of every x-ray unit sold. And here's dollars-and-cents proof of what GE quality means to you in just one instance.

Take a look at the table above. It's based on actual users' reports of GE kenotron valve tube life. Compare this record with yours.

And remember, it's not just the amount you pay for a new tube—although even the "cheap" ones cost around \$100.00! You must also consider the inconvenience to your patients . . . the upsetting of schedules . . . the cost of a service-man's call.

GE x-ray-equipped offices have learned to take kenotrons' long life for granted. Contrast this with many users of other equipment who find it a matter of routine to replace valves every 12 to 18 months.

This amazing story of kenotron life is not an isolated instance. It's typical of all GE x-ray equipment. Ask your GE x-ray representative to show you how your equipment dollars go farther when you buy GE quality. Phone or write the nearest office of General Electric X-Ray Corp., Ltd.—Montreal, Toronto, Vancouver, Winnipeg.

You can put your confidence in —

**GENERAL**  **ELECTRIC**

?

r  
s  
ed

n  
y  
s  
y

n  
e

u  
",  
i-  
c  
e-

o  
st  
o  
y

n  
y  
o  
er  
ne  
",  
g.

C